AWARD NUMBER: W81XWH-20-1-0048

TITLE: Fusogen Nanomedicine for Peripheral Nerve Repair

PRINCIPAL INVESTIGATOR: Joachim Kohn, PhD

CONTRACTING ORGANIZATION: Rutgers, The State University of New Jersey
New Brunswick, NJ

REPORT DATE: January 2021

TYPE OF REPORT: Annual Report

PREPARED FOR: U.S. Army Medical Research and Materiel Command
Fort Detrick, Maryland 21702-5012

REPORT DOCUMENTATION PAGE

Form Approved
OMB No. 0704-0188

1. REPORT DATE	**2. REPORT TYPE**	**3. DATES COVERED**
January 2021	Annual	01Jan2020-31Dec2020

4. TITLE AND SUBTITLE

Fusogen Nanomedicine for Peripheral Nerve Repair

5a. CONTRACT NUMBER
W81XWH-20-1-0048

5b. GRANT NUMBER

5c. PROGRAM ELEMENT NUMBER

6. AUTHOR(S)

Joachim Kohn, PhD, David I Devore, PhD; Cemile Bektas, PhD; Daniel Chakhalian, MD; Kim-phuong Le, PhD; Mariana Lima, BS; Yong Mao, PhD; Antonio Merolli, MD; Joseph M Rosen, MD

E-Mail:kimphuong.le@rutgers.edu; didevore@gmail.com

5d. PROJECT NUMBER

5e. TASK NUMBER

5f. WORK UNIT NUMBER

7. PERFORMING ORGANIZATION NAME(S) AND ADDRESS(ES)

RUTGERS, THE STATE UNIVERSITY OF NEW JERSEY
3 RUTGERS PLZA
NEW BRUNSWICK NJ 08901-8559

8. PERFORMING ORGANIZATION REPORT NUMBER

9. SPONSORING / MONITORING AGENCY NAME(S) AND ADDRESS(ES)

U.S. Army Medical Research and Development Command
Fort Detrick, Maryland 21702-5012

10. SPONSOR/MONITOR'S ACRONYM(S)

11. SPONSOR/MONITOR'S REPORT NUMBER(S)

12. DISTRIBUTION / AVAILABILITY STATEMENT

Approved for Public Release; Distribution Unlimited

13. SUPPLEMENTARY NOTES

14. ABSTRACT

This project is directed at the PRMRP Focus Area of development of novel therapies to repair neurosensory damage. The project deliverables are fusogenic nanoparticles (FNPs), comprised of polymeric fusogens (biomaterials that enhance cell membrane fusion) and cholesterol, to synergistically repair injured peripheral nerves. The central hypothesis being tested is that a systematic exploration of structure-function relationships among novel amphiphilic tyrosine-derived block copolymer surfactants (TyPS) can lead to significantly more effective FNPs which will allow immediate re-establishment of axonal continuity and function. This is being enabled by the first thermodynamically-based systematic exploration of structure-activity relations for polymeric fusogens. Concurrently, controlled delivery of cholesterol, a natural membrane component with fusogenic properties which is being encapsulated in the TyPS-based FNPs, is for the first time being investigated for repair of severed nerves. The rationale for this project is that, after injuries involving the transection of nerves, anatomical recovery is usually incomplete due to inherently slow nerve regrowth rates and rapid proximal and distal (Wallerian) degeneration of the stumps. Consequently most patients can suffer substantial life-long disability and even chronic pain if a neuroma follows. Among combat wounded US military personnel, nerve injuries are a leading cause of unfitting conditions and each year over 100,000 civilian trauma patients suffer disabling nerve injuries which incur enormous long-term healthcare costs. There are currently no fusogens useful for nerve repair approved by the US Food and Drug Administration.

15. SUBJECT TERMS
None listed.

16. SECURITY CLASSIFICATION OF:			**17. LIMITATION OF ABSTRACT**	**18. NUMBER OF PAGES**	**19a. NAME OF RESPONSIBLE PERSON**
					USAMRMC
a. REPORT	**b. ABSTRACT**	**c. THIS PAGE**	Unclassified		**19b. TELEPHONE NUMBER** *(include area code)*
Unclassified	Unclassified	Unclassified			

TABLE OF CONTENTS

1. INTRODUCTION:

Nerve damage, including crushed and severed nerves, is one of the most frequent and debilitating injuries suffered in combat as well as in civilian trauma cases. Current methods of nerve repair include surgical suturing (direct end-to-end coaptation) or nerve grafts depending on the injury gap distance between distal and proximal nerve stumps. In either case, axonal regeneration is a slow process and functional recovery is dependent on the site of injury and the type of treatment, being slow, poor or absent in the worst cases. Several polymers such as poly(ethylene glycol) (PEG) have been found to act as fusogens (defined as biomaterials which enhance the fusion of cell membrane). The proposed research will, for the first time, provide a thermodynamically-based systematic exploration of structure-activity relations for polymeric fusogens comprised of synthetically tunable tyrosine-derived polymeric surfactants (TyPSs). The controlled delivery of cholesterol with TyPS-based fusogen nanoparticles (FNPs) will also, for the first time, be investigated for the repair of axonal membranes. The FNPs will then be applied to in vivo nerve repair to better characterize the relationship between fusogenicity and electrophysiological and histological outcomes.

2. KEYWORDS:

fusogens; peripheral nerve repair; tyrosine-derived polymeric surfactants; cholesterol; nanoparticles; hydrophile:lipophile balance; cytotoxicity; hemolysis; dorsal root ganglia

3. ACCOMPLISHMENTS:

What were the major goals of the project?

The study design consists of three Specific Aims. In **Aim 1, Formulation and biophysical properties of FNPs,** diblock and triblock tyrosine-derived polymeric surfactants (TyPSs) have been designed and synthesized based on calculated thermodynamic properties (hydrophile-lipophile balance (HLB) and Hildebrandt-Hansen solubility parameters), evaluated for insertion in model phospholipid membranes and formulated into self-assembled TyPS-cholesterol fusogen nanoparticles (FNPs) which have been characterized for particle size and cholesterol binding levels. In **Aim 2, Evaluation of FNP in vitro axonal membrane repair and cytotoxicity,** a fluorochrome dynamics methods has been developed to measure axon fusion in severed rat dorsal root ganglia (DRG) membranes treated with the FNPs, PEG and Poloxamer 188; TyPS were demonstrated to be non-cytotoxic to human dermal microvascular endothelial cells; and, flow cytometry was used to demonstrate improved cell viability with rat B35 neuroblastoma cells. In **Aim 3, Evaluation of the lead FNP in an in vivo rat tibial (sciatic - tibial branch) nerve injury model,** the US Army Animal Care and Use Review Office (ACURO) has approved our protocol for the in vivo evaluation of the FNPs for repair of severed tibial nerves, with electrophysiological and histological outcomes used to determine the relative treatment efficacies of the known fusogens poly(ethylene glycol) (PEG) and Poloxamer 188 (a commercial block copolymer surfactant) and the selected FNP injected at the surgical site. The status of the tasks and milestones in the Statement of Work are summarized in the table below.

Specific Aim 1: Formulation and biophysical properties of Fusogen Nanoparticles (FNPs)	Timeline Months	Status
Major Task 1: Design and synthesis of tyrosine-derived block copolymer surfactants (TyPSs)	1-2	
Subtask 1.1: Thermodynamic calculations of Hoy solubility parameters and Hydrophile:Lipophile Balances (HLBs) for TyPSs over the statistically designed parameter ranges	1-2	Complete
Subtask1 2: Synthesis and structural characterization of a library of 16 initial TyPSs	1-2	Initial set of triblock and diblock TyPS synthesized, characterized; additional sets to be prepared after in vitro cell studies completed
Milestone: TyPSs' compositions confirmed by ^{1}H NMR and GPC	2	Completed for initial set of TyPS
Major Task 2: Biophysical properties of TyPSs	3-5	
Subtask 2.1: Determine surface tensions and critical aggregation concentrations (CACs) of TyPSs in PBS	3-4	Complete
Subtask 2.2: Determine Langmuir film balance surface pressure/surface area properties for TyPS, PEG and P188 insertion in DPPC, DPPG and PS phospholipid films	4-5	Complete
Milestone(s): Structure-property relations determined for TyPSs based on their solubility parameters, HLBs, CACs and surface pressure/surface area responses	5	Complete; TyPS insert in Langmuir phospholipid films
Major Task 3: Biophysical properties of FNPs	5-8	
Subtask 3.1: Prepare self-assembled FNPs of each TyPS and cholesterol and determine particle sizes, zeta potentials and stabilities as a function of cholesterol loading/binding levels	5-6	Completed for initial set of TyPS
Subtask 3.2: Determine cholesterol release kinetics from the FNPs in PBS	6-7	Complete for initial set of TyPS
Subtask 3.3: Determine $\log_{10}$P(o/w) for the FNPs	6-7	In progress (50% complete)
Milestones: Correlation of FNP properties with TyPS properties; Identification and synthesis of additional TyPS compositions based on Stat-Ease statistical design analysis for optimized FNP	8	Complete for initial set of TyPS

biophysical properties		
Major Task 4: IACUC and ACURO animal protocol reviews	4-12	
Subtask 4.1: Document rat tibial nerve protocol surgical procedure, animal care and safety, and experimental design; submit to Rutgers IACUC and US Army ACURO	4-6	Complete
Milestones: IACUC and ACURO approvals of rat nerve injury protocol	12	Complete
Specific Aim 2: Evaluation of FNP *in vitro* axonal membrane repair and cytotoxicity.		**Site 1**
Major Task 5: FNP repair of DRG axon membranes		
Subtask 5.1: Compare the efficacy of FNPs, PEG and P188 for fusion of severed DRG axon fusion based on fluorochrome dynamics	7-12	DRG method development complete; TyPS testing initiated, 30% complete
Subtask 5.2: Determine the efficacy of FNPs for delivery of cholesterol to DRG axonal membranes based on quantitative HPLC analysis	12-16	Experiments initiated; 0% complete
Major Task 6: Cytotoxicity of FNPs		
Subtask 6.1. Determine the cytotoxicity of FNPs, TyPSs, PEG and P188 based on MTT viability assays for HECs and primary nerve cells	14-16	Complete
Subtask 6.2: Determine the hemolytic activity of FNPs, TyPS, PEG and P188	14-16	Method development complete; HRPO approval requested; FNP evaluations 0% complete
Milestone: Structure-performance relations determined for FNP repair of severed DRG axons and for cytotoxicities; Lead candidate FNP identified for Aim 3 *in vivo* studies	16	TyPS and FNPs exhibit minimal cytotoxicity; DRG studies initiated; lead candidate to be selected in first quarter 2021
Specific Aim 3: *Evaluation of the lead FNP in an in vivo rat tibial nerve injury model.*		
Major Task 7: Determine relative efficacies of FNPs, PEG and P188 for repair of severed tibial nerves	17-24	
Subtask 7.1: Obtain pre-injury compound action potentials, perform surgical tibial nerve	17-19	To be initiated by 2nd quarter 2021; 0% complete

transections, inject fusogens (TyPS-cholesterol FNP, P188-cholesterol and PEG) at the surgical sites and surgically repair the nerves		
Subtask 7.2: One week post-injury, obtain post-injury compound action potentials and then euthanize the animals	20-21	To be initiated by 2nd quarter 2021; 0% complete
Subtask 7.3: Retrieve 20mm segments of distal and proximal tibial nerves, perform histological analysis of axon populations and conduct statistical analyses of *in vivo* data	21-23	To be initiated by 2nd quarter 2021; 0% complete
Milestones achieved: Relative fusogenic performance of FNPs and PEG determined; Final report submitted to DoD; Manuscript(s) submitted to journals; Patent applications filed	24	To be initiated by 2nd quarter 2021; 0% complete

What was accomplished under these goals?

The objectives, significant results and key outcomes for each of the Specific Aims and Tasks outlined in the project Statement of Work (SOW; see above Table) are provided here in the order they appear in the SOW. Most but not all of the Tasks which were targeted for completion in Year 1 of the project were fully or at least partially completed. Some delays were caused by University-imposed restricted access to our laboratories between March and July, 2020, due to the COVID-19 pandemic, which slowed by never fully stopped our work. Those few Year 1 tasks which were not fully completed are in progress and anticipated to be completed in the first quarter of 2021.

The project team has met biweekly since January, 2020, (initially in person and via Zoom since March) to assure collaborative planning and data reviews.

In Year 1, several key outcomes were achieved: 1) thermodynamic solubility parameters and hydrophile;lipophile balances (HLBs) were calculated for a wide range of tyrosine-derived polymeric surfactants (TyPSs) which provided systematic estimates of TyPS ability to bind cholesterol and to interact with cell phospholipid membranes; 2) an initial set of TyPSs were synthesized based on their predicted thermodynamic properties and were demonstrated to self-assemble into functional nanoparticles (FNPs) having a narrow range of diameters appropriate for injectable nanomedicines; 3) the TyPSs inserted into Langmuir phospholipid monolayer films and their FNPs effectively bound significant levels of cholesterol; 4) the TyPS were non-cytotoxic to human dermal cells and caused the fusion of rat B35 neuroblastoma cells while improving their viability; and, 5) new in vitro methods for cutting and detecting the fusion in vitro at single axon level in dorsal root ganglia were developed.

Specific Aim 1: Formulation and biophysical properties of Fusogen Nanoparticles (FNPs)

Task 1. Design and synthesis of tyrosine-derived block copolymer surfactants (TyPS).

1.1.Thermodynamic property calculations. To determine if predictive structure-property relations can be developed for polymeric fusogens, solubility parameters and surfactant properties of tyrosine-derived block copolymer surfactants (TyPS), poly(alkylene oxides) (i.e., poly(ethylene oxide) (PEO) and poly(propylene oxide) (PPO)) and their block copolymers were calculated using established thermodynamic methods. The synthetically tunable tyrosine-derived copolymer surfactants (TyPS) were "A-B-A" triblocks and "A-B" diblocks comprised of a hydrophobic desaminotyrosyl tyrosine -diacid (DTR-XA) B-block and either one or two hydrophilic poly(ethylene oxide) A-blocks (Figure 1).[1,2,3] The thermodynamic properties were also calculated for comparable commercial triblock copolymer surfactants, known as Poloxamers™ or Pluronics™, which are comprised of PEO_n-PPO_m-PEO_n..

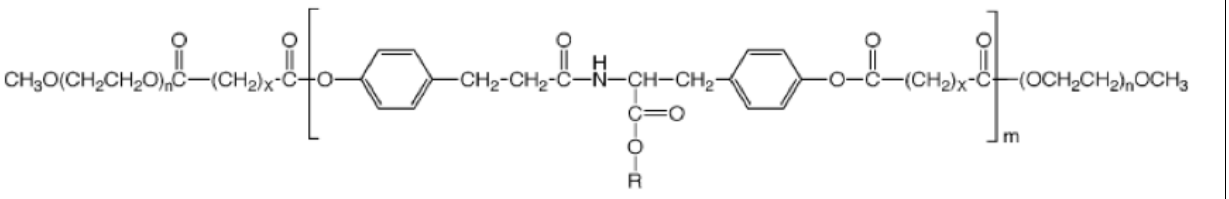

Figure 1. Tyrosine-derived block copolymer surfactant (TyPS) structure. Synthetically tunable composition variables include: the molecular weight (degree of polymerization) of the end-cap hydrophilic poly(ethylene oxide) (PEO) A-block(s) chains (n); the diacid alkyl chain length (x); the pendent alkyl ester chain length (R); and the molecular weight (degree of polymerization) of the hydrophobic oligoDTR-XA B-block (m).

TyPSs have been demonstrated to self-assemble in aqueous solutions into core-shell nanospheres ("Tyrospheres") with typical hydrodynamic diameters of 70 to 100nm and with very low critical aggregation concentrations (CACs) on the order of 10^{-6} g/mL. [1,4] Tyrospheres bind and encapsulate predominantly hydrophobic molecules such as paclitaxel, campothecin and curcumin in the hydrophobic B-block core by non-covalent binding and effectively controlled the release kinetics of the hydrophobic drug cargoes in vitro and in vivo.[4-6]

Polymer binding of hydrophobic molecules can be predicted using Flory-Huggins theory (Equation 1) [7]:

$$\Delta G_m/RT = n_d \ln\varphi_d + n_p \ln\varphi_p + n_d \varphi_p \chi_{dp} \qquad (1)$$

where ΔG_m is the free energy of mixing, n_d is the number of moles of component 1 (e.g., a cargo drug such as paclitaxel or cholesterol), n_p is the number of moles of component 2 (e.g., the TyPS copolymer), the φ_i are their respective volume fractions.

The Flory-Huggins interaction parameter χ is given by

$$\chi \sim (V_1/RT)\,[\partial(\text{cholesterol}) - \partial(\text{triblock copolymer})]^2 \quad (2)$$

where the solubility parameters, ∂, are related to the cohesive energy density (E_{coh}) by

$$\partial = (E_{coh}/V)^{1/2} \quad (3)$$

and where compatibility (solubility) increases as $\chi \rightarrow 0$.[7]

Solubility parameters can be determined experimentally by several methods including, for simple organic solvents, from their heats of evaporation and, for polymers from their relative swelling, intrinsic viscosities or dissolution in a series of solvents of known cohesive energy densities.[8] Alternatively, solubility parameters can be calculated from the known molecular structures using component group contribution values.[8-10] Several different component group contribution approaches have been developed; all assume that group contributions are linearly additive. Improvement in the correlation between experimentally measured and theoretically calculated solubility parameters were made by Hansen by decomposing ∂_T into dispersive (∂_d), polar (∂_p) and hydrogen bonding (∂_h) factors (equ.8-11) [10]:

$$\partial_T^2 = \partial_d^2 + \partial_p^2 + \partial_h^2 \text{ , where} \quad (8)$$
$$\partial_d = \sum F_{di} / V \quad (9)$$
$$\partial_p = (\sum F_{pi}^2)^{1/2} / V \quad (10)$$
$$\partial_h = (\sum E_{hi}/V)^{1/2} \quad (11)$$

For a copolymer comprised of monomers “a” and “b” (e.g., for TyPS, a= PEO and b = DTR-XA), the solubility parameter ∂_{ab} can be calculated from the volume fraction (or weight fraction) of the components [11]:

$$\partial_{ab} = \partial_a \varphi_a + \partial_b \varphi_b \quad (12)$$

Solubility parameters for selected TyPS hydrophobic B-blocks, poly(ethylene oxide) (PEO), poly(propylene oxide) (PPO) and cholesterol (Figure 2) were calculated from equations 8-12 using the group contribution values of Hoftyzer and van Krevelen [8,9] and are summarized in Table 1:

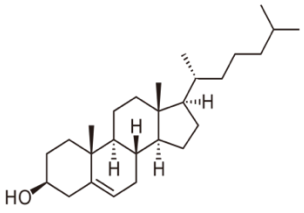

Figure 2. Cholesterol

Table 1. Calculated Hansen solubility parameters.
Solubility parameter units $(Jcm^{-3})^{1/2}$.

	∂_d	∂_p	∂_h	∂_T
DTE-SA	17.40	2.78	7.85	19.29
DTO-SA	17.40	3.44	7.11	19.11
DTD-SA	17.39	2.03	6.72	18.75
DTD-DA	17.39	1.83	6.38	18.61
PEO	17.04	10.65	8.94	21.99
PPO	15.44	5.82	8.94	17.78
Cholesterol	16.14	1.32	7.27	17.75

The solubility parameters calculated here for cholesterol, PEO and PPO were in good agreement with their published experimental values: cholesterol, ∂_T =18.4 [12]; PEO, ∂_T = 22.9 [7] and 22.0 [13]; and, PPO, ∂_T =18.5 [14].

The solubility parameters for selected diblock and triblock TyPSs and P188 were calculated using equation 12 with the Hansen parameters from Table 1 and the weight fractions of the A-blocks and

B-blocks, φ_a and φ_b, respectively, and were summarized in Table 2. The Flory-Huggins interaction parameters with cholesterol and with the membrane phospholipid 1,2-Dipalmitoyl-sn-glycero-3-phosphoglycerol (DPPG) were then calculated using equation 2 and were summarized in Table 2.

Table 2. Copolymer solubility parameters (∂_T) and Flory-Huggins interaction parameters (χ) for copolymers with cholesterol and membrane phospholipid DPPG.

	φ_a (PEO block)	φ_b (DTR-XA or PPO block)	∂_T $(Jcm^{-3})^{1/2}$	χ Polymer/ cholesterol (298°K)
Cholesterol	-	-	17.75	-
Dipalmitoylphosphatidylglycerol (DPPG)	-	-	20.24	
PEO	1.0	0	21.99	2.73
PPO	0	1.0	17.78	0.0
PEO_{80}-PPO_{27}-PEO_{80} (P188)	0.817	0.183	21.22	1.83
PEO(5k)-$(DTE\text{-}SA)_{12}$-PEO(5k)	0.617	0.383	20.96	1.57
PEO(5k)-$(DTO\text{-}SA)_{10.5}$-PEO(5k)	0.617	0.383	20.89	1.50
PEO(5k)-$(DTD\text{-}DA)_{10.5}$-PEO(5k)	0.617	0.383	20.70	1.32
PEO(2k)-$(DTD\text{-}DA)_{10.5}$-PEO(2k)	0.392	0.608	19.93	0.722
PEO(5k)-$(DTE\text{-}SA)_{24}$-PEO(5k)	0.454	0.545	20.55	1.57
PEO(5k)-$(DTO\text{-}SA)_{27}$-PEO(5k)	0.358	0.642	20.14	0.868
PEO(5k)-$(DTD\text{-}SA)_{23}$-PEO(5k)	0.407	0.593	20.07	0.818
PEO(5k)-$(DTE\text{-}SA)_{24}$	0.294	0.706	20.08	0.825
PEO(5k)-$(DTO\text{-}SA)_{27}$	0.218	0.782	19.74	0.602
PEO(5k)-$(DTD\text{-}SA)_{23}$	0.255	0.745	19.58	0.509

It could therefore be predicted, based on compatibility increasing as $X \rightarrow 0$, that cholesterol would have the highest affinity for the most hydrophobic TyPS B-block, DTD-DA, and would also have high affinity for the PPO block of a triblock copolymer such as Poloxamer 188 (P188) comprised of PEO_{80} -PPO_{27} -PEO_{80}. However, the hydrophilic A-blocks of the TyPS and P188 significantly altered the anticipated affinity for cholesterol, as reflected in the relatively large Flory-Huggins parameter value for P188 (1.83) compared to those of the TyPS diblocks (0.509 to 0.82) and TyPS triblocks (0.722 to 1.57). It could also be predicted that the triblock TyPS comprised of PEO(5k)-$(DTO\text{-}SA)_{27}$-PEO(5k) and PEO(5k)-$(DTD\text{-}SA)_{23}$-PEO(5k), which were abbreviated as (T-DTO) and (T-DTD), would have the greatest binding affinity with the phospholipid DPPG and would therefore strongly insert into cell bilayer membranes comprised of DPPG and similar phospholipids.

The surface activity of the surfactants in aqueous solutions have typically been characterized by calculating their hydrophile:lipophile balance (HLB) values, which were originally defined by Davies' empirical group contribution method [15,16]:

$$HLB = 7 + \sum(\text{hydrophilic group numbers}) + \sum(\text{hydrophobic group numbers}) \qquad (13)$$

The HLB group numbers, while empirical, were based on the free energy change for transferring the organic functional group (e.g., - CH_2 -, -COOH, etc.) from an aqueous phase to an oil phase, and at least within a family of related surfactant structures they have been related to the critical

aggregation concentrations (CACs) [17]:

$$\log CAC = a + b\ HLB \quad (14)$$

For surfactants comprised of PEO and PPO chains or long alkyl chains, the Davies group numbers tended to provide incorrect estimates of surfactant behavior. Modifications of the group numbers have therefore been introduced by Guo, et al [18] to account for the "effective chain lengths" of the PEO, PPO and alkyl chains, and the more realistic HLB values were then obtained by Guo's equations15-19:

$$HLB = 7 + GN(CH_2) \times N(CH_2,eff) + GN(EO) \times N_{(EO,eff)} + GN(PO) \times N_{(PO,eff)} + \sum GN(\text{other hydrophilic groups}) + \sum GN(\text{other lipophilic groups}) \quad (15)$$

where GN=group number and N=number of the functional group in the molecule,

$$N_{(PO,eff)} = 2.057N(PO) + 9.06 \quad (16)$$

$$N_{(EO,eff)} = 13.45 \ln(N_{EO}) - 0.16N_{EO} + 1.26, \quad 1 \le N_{EO} \le 5 \quad (17)$$

$$N_{(EO,eff)} = 0.056N_{EO} + 43.08 \qquad N_{EO} \ge 50 \quad (18)$$

$$N_{(CH2,eff)} = 0.965N_{CH2} - 0.178 \quad (19)$$

The HLBs for prototype TyPSs, P188 and similar PEO-PPO-PPO triblocks, and cholesterol were calculated using equations 15-19 and were summarized in Table 3:

Table 3. Calculated HLB values.

Composition	HLB
PEO(2k)-(DTE-SA)$_{12}$-PEO(2k)	60.8
PEO(5k)-(DTE-SA)$_{12}$-PEO(5k)	63.6
PEO(2k)-(DTO-SA)$_{10.5}$-PEO(2k)	28.9
PEO(5k)-(DTO-SA)$_{10.5}$-PEO(5k)	31.7
PEO(5k)-(DTD-SA)$_{10.5}$-PEO(5k)	12.4
PEO(5k)-(DTD-DA)$_{10.5}$-PEO(5k)	-7.50
PEO(5k)-(DTE-SA)$_{24}$-PEO(5k)	87.5
PEO(5k)-(DTO-SA)$_{27}$-PEO(5k)	19.3
PEO(5k)-(DTD-SA)$_{27}$-PEO(5k)	-19.9
PEO(5k)-(DTE-SA)$_{24}$	71.2
PEO(5k)-(DTO-SA)$_{27}$	2.90
PEO(5k)-(DTD-SA)$_{23}$	-36.2
(P188) PEO$_{80}$-PPO$_{27}$-PEO$_{80}$	28.7
(P85) PEO$_{26}$-PPO$_{40}$-PEO$_{26}$	24.3
(F88) PEO$_{103}$-PPO$_{39}$-PEO$_{103}$	25.8
(P105) PEO$_{37}$-PPO$_{56}$-PEO$_{37}$	17.3
(F127) PEO$_{100}$-PPO$_{65}$-PEO$_{100}$	17.7
Cholesterol	-2.93

As expected, as the degree of polymerization (dp) of the TyPS PEO A-blocks increased from 2kDa to 5kDa at constant B-block length, the copolymer HLB increased. (For the prototype TyPS with

PEO(2kDa), the PEO dp = 2,000/44 = 45, and for TyPSs with PEO(5kDa), the dp = 5,000/44= 114.) And as the hydrophobicity of the TyPS B-block increased (i.e., as quantified in Table 1, DTD>DTO>DTE) the HLB decreased. The HLB calculated for P188 using the Guo, et al, equations was 28.7, which was in good agreement with the reported experimental value of 29; other published experimental HLB values for the Pluronics F88 (HLB=28), P105 (HLB=15) and F127 (HLB=22) were also in good agreement [19] but the experimental value for P85 (HLB=15) was not, perhaps due to a significant amount of diblocks which might be present in the commercial product.

1.2. Synthesis and structural characterization. An initial set of three diblock and three triblock TyPSs were synthesized using our established carbodiimide coupling reaction process. The tyrosine-derived monomers which comprised these TyPS were: DTE (desaminotyrosyl-tyrosine ethyl ester); DTO (desaminotyrosyl-tyrosine octyl ester); and, DTD (desaminotyrosyl-tyrosine dodecyl ester). The esters were made with suberic acid (SA) to form DTE-SA, DTO-SA and DTD-SA monomers, which were then polymerized using standard condensation reactions and end-capped at either one terminal end (to form the diblocks) or both terminal ends (to form the triblocks) with poly(ethylene glycol) methyl ether 5 kDa (mPEG(5k)) (Figure 3).

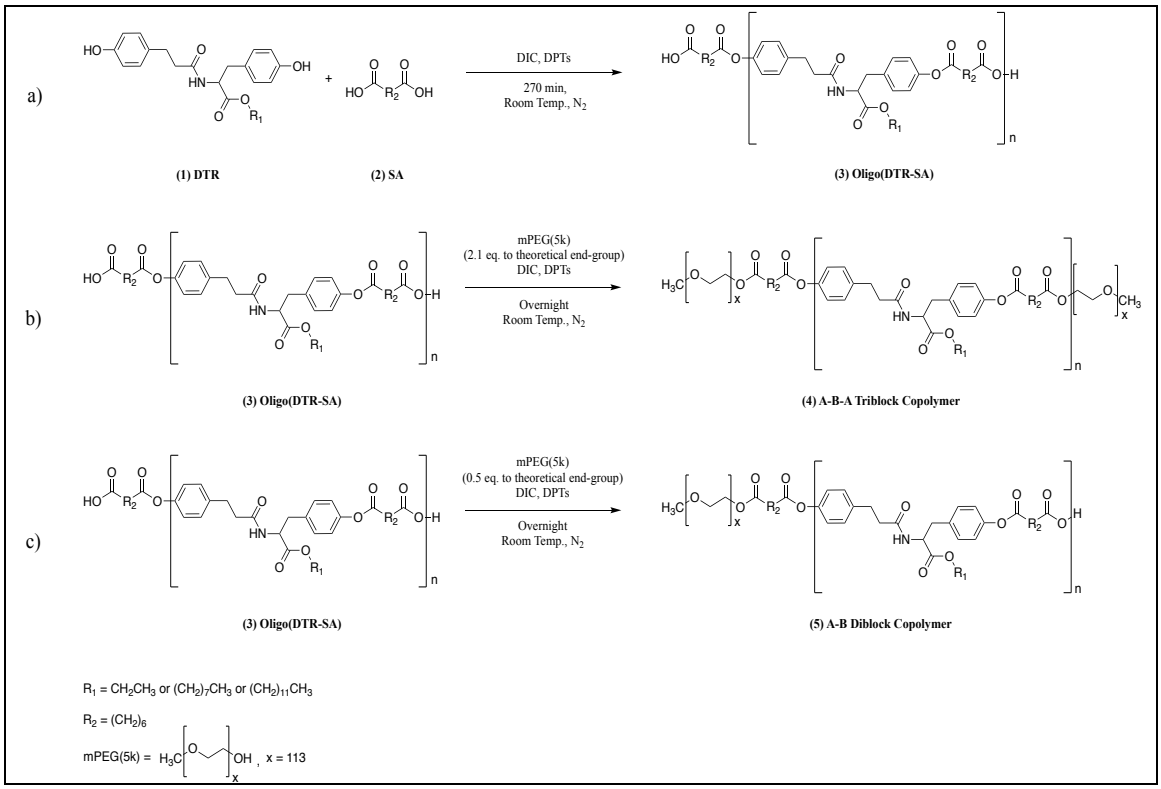

Figure 3. Synthesis scheme for diblock and triblock tyrosine-derived polymeric surfactants (TyPSs).

The DTR-SA blocks provided hydrophobic properties while the PEG blocks provided hydrophilic properties to these amphiphilic copolymers. Diblocks and triblocks with identical hydrophobic blocks were synthesized in order to compare their surfactant properties, including self-assembly into nanoparticles and their cholesterol encapsulation efficiencies. Prior research [20] had shown substantial systematic differences in those thermodynamic properties for diblock and triblock poly(alkylene oxide) polymeric surfactants based on analogous structures to the TyPS but comprised of poly(propylene oxide) (PPO) hydrophobic blocks with hydrophilic PEG (aka

poly(ethylene oxide) (PEO)) blocks. Those differences were driven by the folding of the hydrophobic blocks in the triblocks, driven by molecular van der Waals forces and the relative physical size exclusion properties of the hydrophilic "head" groups and hydrophobic "tail" groups. Molecular mechanics studies previously performed by our group of TyPS structures was consistent with this picture of the folding of the hydrophobic DTR-SA blocks in aqueous solutions [4].

The molecular compositions of the synthesized TyPSs were confirmed by proton nuclear magnetic resonance (^{1}H-NMR) using a Varian VNMRS 500 MHz spectrophotometer and their molecular weights and molecular weight distributions were determined by gel permeation chromatography (GPC) using a mobile phase of tetrahydrofuran (THF)/butylated hydroxytoluene (BHT) and a refractive index detector (Table 4).

Table 4. TyPS molecular weight, polydispersity index (PDI) and degree of polymerization of tyrosine-derived hydrophobic (oligo(DTR-SA)) block.

Polymers	M_n (kDa)	M_w (kDa)	PDI	Oligo(DTR-SA) DP*
T-DTE	20.09 (0.05)	24.31 (0.03)	1.210 (0.001)	24
T-DTO	22.69 (0.01)	27.25 (0.05)	1.201 (0.002)	25
T-DTD	21.73 (0.06)	26.09 (0.06)	1.201 (0.001)	24
D-DTE	12.17 (0.02)	17.26 (0.01)	1.418 (0.003)	25
D-DTO	16.79 (0.03)	22.35 (0.03)	1.331 (0.001)	24
D-DTD	16.71 (0.05)	21.04 (0.04)	1.259 (0.003)	24

T: Triblock. D: Diblock. mPEG(5kDa) in all cases. M_n: number-average molecular weight. M_w: weight-average molecular weight. PDI: polydispersity index. DP: Degree of polymerization of the oligo(DTR-SA) block. Three separate batches of each TyPS were synthesized; the standard deviations of the independent triplicates are in parenthesis.

Task 2. Biophysical properties of TyPS.

2.1. Surface tension and critical aggregation concentration (CAC). The critical aggregation concentration (CAC) (aka critical micelle concentration, CMC) for each TyPS was determined by measuring the change in fluorescence of the dye Nile red in the bound (aggregate) state compared to the unbound state.[21] Surface tension measurements were not pursued due to the extremely low CAC values for the TyPS which could not be clearly determined by the traditional DuNouy tensiometer method. A range of 24 concentrations was used for each TyPS in phosphate buffered saline (PBS; pH7) from 9 x 10^{-2} µg/mL to 10 µg/mL. Fluorescence intensity scans were obtained at 25°C using a TECAN Spark multimode microplate reader with excitation wavelength set at 550nm and emission wavelength of 635 nm. The CAC was taken as the inflection point of data plotted as emission intensity versus log time. All of the diblock and triblock TyPS were found to self-assemble at very low concentrations (Table 5).

Table 5. Critical aggregation concentrations of TyPS in PBS at 25ºC. TyPS CACs were determined with Nile red probe at 25ºC; Pluronic CACs determined with pyrene probe at 37ºC[19]

TyPS	CAC (mM)
T-DTE: PEO(5k)-(DTE-SA)$_{24}$-PEO(5k)	0.027
T-DTO: PEO(5k)-(DTO-SA)$_{27}$-PEO(5k)	0.028
T-DTD: PEO(5k)-(DTD-SA)$_{23}$-PEO(5k)	0.020

D-DTE: PEO(5k)-(DTE-SA)$_{24}$	0.063
D-DTO: PEO(5k)-(DTO-SA)$_{27}$	0.017
D-DTD: PEO(5k)-(DTD-SA)$_{23}$	0.030
(P188;F68): PEO_{80}-PPO_{27}-PEO_{80}	0.48
(P85): PEO_{26}-PPO_{40}-PEO_{26}	0.065
(F88): PEO_{103}-PPO_{39}-PEO_{103}	0.25
(P105): PEO_{37}-PPO_{56}-PEO_{37}	0.001
(F127): PEO_{100}-PPO_{65}-PEO_{100}	0.006

No strong systematic relationship between the TyPS compositions and their experimental CACs was observed. The value obtained here for the T-DTO was in reasonably good agreement with experimental values which our group previously obtained for similar TyPS with different B-block degrees of polymerization: CAC= 0.26 µg/mL using static light scattering [1] and 2.2 µg/mL using pyrene fluorescence measurements.[4] It is noted that CAC values for the Pluronics have been obtained by several different research groups using diverse methods (fluorescent probe binding and light scattering) and there is poor agreement between those published values.[19] For the Pluronics (Poloxamers), it has been shown that the CAC values are inversely proportional to the temperature and there is no reported CAC for P188 at 25°C. In contrast, the TyPS all self-assemble at 25°C with very low CACs.(Table 5).

In contrast to the TyPS, the CAC for P188 has been found to be orders of magnitude greater; i.e., P188 is far less surface active than the TyPSs. Our group previously found using pyrene fluorescence that the CAC for P188 is 0.44mg/mL at 37°C [4] and an even higher CAC of 4.0mg/mL obtained by similar pyrene fluorescence at 37°C has been reported.[22] The P188 CAC determined by Langmuir trough surface pressure was reported to be 0.125mM (1.0 mg/mL) at 30°C.[23] Although these P188 CACs reflect commonly observed experimental variations, it was clear that the TyPS self-assembled at far lower concentrations than P188. That observation was consistent with thermodynamic theory [20] which predicted that the CACs would be directly related to the copolymer solubility parameters as can been seen from the calculated ∂_T values in Table 2.

2.2. Langmuir film balance (LFB) measurement of surface pressure – mean molecular area (π–A) isotherms. Poloxamer 188 has been shown to insert into phospholipid monolayer films at low surface pressures and to diffuse out of the films at high surface pressures.[23] That behavior, which was correlated with the therapeutic effects of P188 on repair of injured muscle and nerve tissue [24], provided the initial impetus for this research project.

The effect of TyPSs on the surface pressure of phospholipid monolayers was determined using a double barrier Langmuir film balance (KSV Minimicro surface balance with an 8400mm^2 single trough, KSV Instruments, Finland) equipped with a microroughened platinum Wilhemy plate (Biolin Scientific/Nanoscience Instrument, USA) and KSV LayerBuilder control software (v.3.3). Filtered phosphate buffer solution (MP Biomedicals, USA) was used as the aqueous subphase at ambient temperature. Phospholipid monolayers were prepared from chloroform solutions of the following three membrane phospholipids:1)1,2-Dipalmitoyl-sn-glycero-3-phospho-rac-(1-glycerol) (DPPG); 2) 1,2-Dipalmitoyl-sn-glycero-3-phosphocholine (DPPC); and, 3) 1,2-Dipalmitoyl-rac-glycero-3-phospho-L-serine,~98% (DPPS) (Sigma-Aldrich, USA). The chloroform solutions at 0.2mg/ml concentration were deposited on the film balance aqueous surface using a glass micro syringe (Hamilton, USA) at a constant volume of 15 microliters to create the phospholipid monolayers. Aqueous TyPS suspension was injected into the film balance subphase using a side port to prevent physical disturbance of the phospholipid monolayer. The compression barrier speed was

kept constant at 20 cm^2/m. Three or more isotherms were collected per each injection.

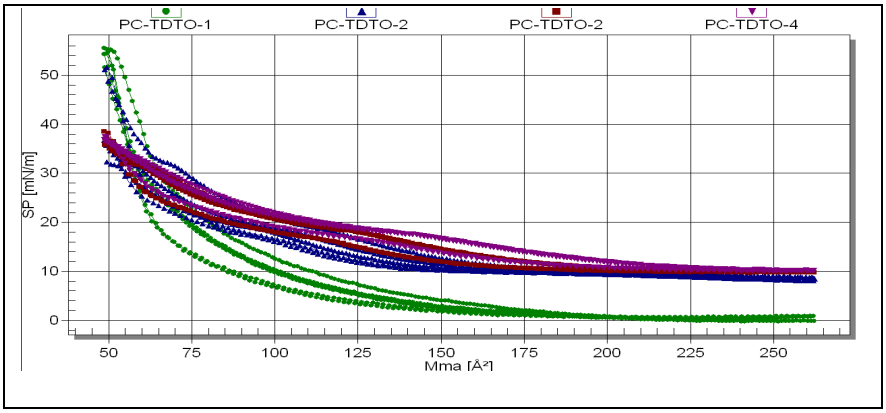

Figure 4. TyPS effect the surface pressure of Langmuir films of DPPC

A typical surface pressure (SP) – surface area isotherm was illustrated in Figure 4 for the DPPC monolayers with the triblock TyPS T-DTO-PEG(5kDa). Some hysteresis was observed as the surface area was compressed (from Mma >250 A^2 to <50 A^2) and then expanded. The surface pressure at a given surface area was significantly increased by the addition of the TyPS, which along with the appearance of multiple surface states (changes in slope as a function of surface area) was indicative of strong insertion of the TyPS into the monolayer film.

The mean molecular area at a fixed surface pressure of 15 mN/m (A_{15}) was obtained from each π–A isotherm to obtain individual Delta A_{15} (Delta) values using equation 20:

$$\Delta A_{15} = A_{15,fusogen} - A_{15,\ Baseline} \qquad (20)$$

Figures 5a-c show the diblock and triblock TyPS insertion behavior in each of the phospholipid monolayers as indicated by Δ, the mean molecular area increases from the respective phospholipid baseline per molecule at a nominal 15 mN/m of surface pressure. This surface pressure was selected for a systematic ranking of the fusogens in this study since no transition occurs around this value for any of the fusogens. In other words, all fusogens are in the same L1 (liquid state) phase at 15 mN/m.

The higher delta values indicate higher degree of stable insertions to the baseline lipid monolayers. While the injection quantities of each of the fusogens varies due to polymer molecular weights and test materials availability, the shape of these Delta – Quantity curves do provide a good prediction toward fusogen stability at higher concentration. At the test conditions, most of the sample groups have not reached the degree of insertion of the control molecule, P188. Table 6 summarizes P188 Delta values for the three lipids.

Table 6: Delta A_{15} (Delta) values for P188 inserted into PC, PS, and PG.

Lipid	PC	PS	PG
Injected Quantity (micromol)	2.98	2.98	2.98
Delta A_{15} (A^2)	188 ± 30	240 ± 2	116 ± 7

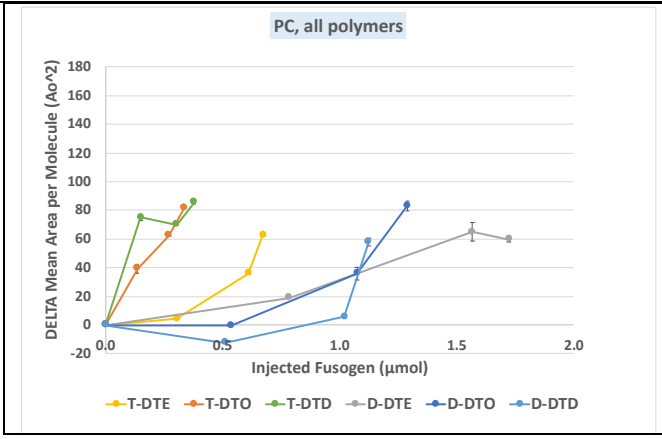

Figure 5a. Stable insertions to PC monolayers are more evident in tri-blocks than di-blocks. D-DTD exhibited a slight negative delta value at its lowest test concentration, most likely due to the lower ability for the polymer to effectively dispersed into the PBS subphase upon injection prior to insertion.

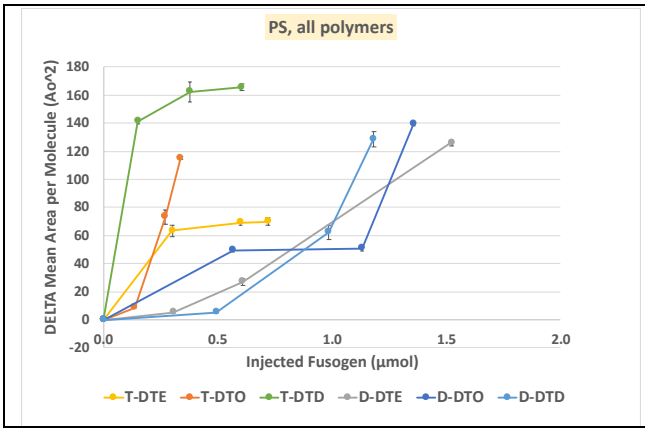

Figure 5b Stable insertions to PS monolayers are more evident in tri-blocks than di-blocks. T-DTE, however, reached a plateau as injection quantity increased.

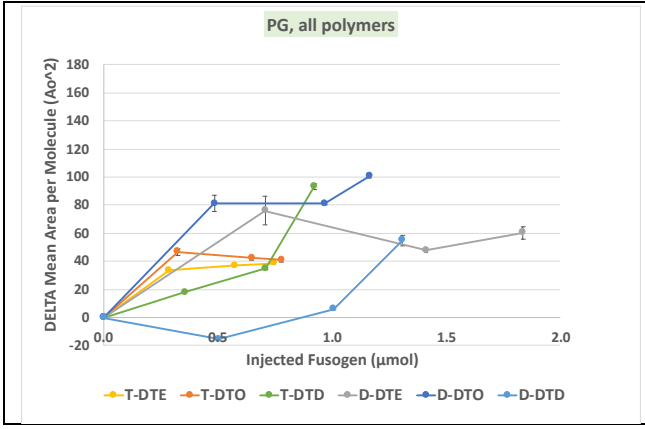

Figure 5c: Insertions into the PG monolayer do not provide as clear a ranking between the tri-blocks and the di-blocks as in the other two lipids.

PEG3.35k also increased the Langmuir film surface pressure (Figure 6) but did not significantly alter the film phase behavior. The increased surface pressure caused by PEG addition was ascribed to the surface adsorption of PEG on the polar head groups of the PC monolayer.

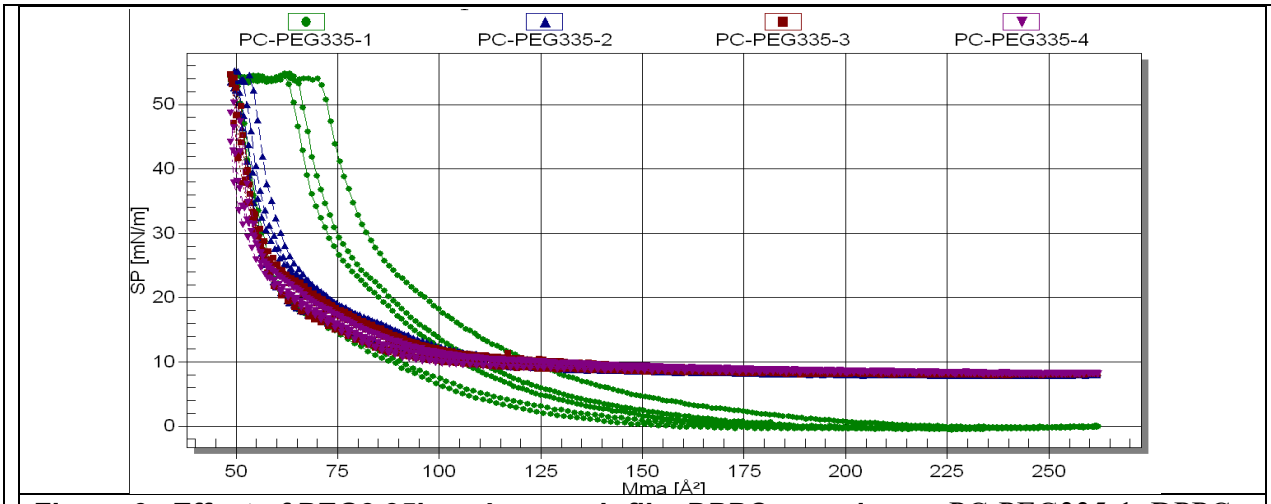

Figure 6. Effect of PEG3.35k on Langmuir film DPPC monolayer. PC-PEG335-1: DPPC baseline (no PEG). PC-PEG-2 to-4 had increasing amounts of PEG3.35k injected into the aqueous subphase.

Task 3. Biophysical properties of Fusogen Nanoparticles (FNPs)

The purpose of preparing nanoparticles loaded with cholesterol was to determine if they would provide controlled delivery of cholesterol to increase its concentration levels in axonal membranes. Cholesterol was known to be a major natural component of eukaryotic cell membranes and acted as a fusogen to modulate membrane fluidity and permeability.[25]

3.1. Fusogen Nanoparticles of tyrosine-derived polymeric surfactants (TyPS) and cholesterol. Nanospheres of unloaded TyPS were prepared using our previously developed nanoprecipitation process.[5] Briefly, the TyPS of interest was dissolved in dimethylformamide (DMF) at 100mg/mL and added dropwise into PBS (pH 7.4) at room temperature under mild stirring. These nanosphere suspensions were filtered through a PVDF syringe filter (0.22 µm or 0.45 µm) and centrifuged in a Beckman Coulter Optima TM L-90K ultracentrifuge (65000 rotations per minute (rpm), 3h, 18 °C). After centrifugation, the supernatant was removed, the pellet was washed twice with PBS and resuspended in PBS overnight under orbital shaking (100 rpm). Each TyPS formulation was prepared in triplicate. Particle size was determined by dynamic light scattering using a Malvern Zetasizer.

Cholesterol loaded nanospheres were also prepared by nanoprecipitation. The TyPS and cholesterol were dissolved in DMF with a range of cholesterol concentrations and added dropwise to PBS (pH7.4) at room temperature. Cholesterol concentrations in the DMF were adjusted to achieve final concentrations in the PBS solution ranging from 1% to 10% wt:vol. The particles sizes of the resultant FNPs were again determined using the Malvern Zetasizer.

Cholesterol binding levels in the FNPs was determined by extraction in isopropyl alcohol (IPA) followed by filtration through a PTFE (0.45 µm) syringe filter. The filtered solution was analyzed by high performance liquid chromatography (HPLC) using a Waters 26695 HPLC system equipped with a UV-Vis Dual 1 absorbance detector (Waters 2487) set at 200 nm and an Agilent Eclipse XDB-C18 (5 µm, 4.6x150 mm) column. The mobile phase was delivered at a flow rate of 1 mL/min, and was composed of a 50:50 mixture of IPA and acetonitrile with addition of trifluoroacetic acid (0.1% v/v). Column temperature was set at 25 °C, and the injection volume at 10 µL. Standard calibration samples were prepared by dissolving cholesterol in IPA in different concentrations ranging from 1 mg/mL to 0.2 mg/mL. Cholesterol concentration was obtained by correlating the

HPLC area under the sample peak with the linear standard calibration curve. Percent loading and loading efficiency were calculated by equations 21 and 22:

$$Loading\ Content = \frac{mass\ of\ encapsulated\ drug}{(mass\ of\ encapsulated\ drug + mass\ of\ the\ recovered\ polymer)} \quad (21)$$

$$Loading\ Efficiency = \frac{mass\ of\ encapsulated\ drug}{mass\ of\ drug\ in\ the\ feed} \quad (22)$$

The hydrodynamic particle properties of the unloaded TyPS nanospheres were summarized in Table 7:

Table 7. Unloaded TyPS nanospheres particle size distributions

Copolymer	Z-Average Size (nm) (n=3)	Average PDI (n=3)	Peak Size (d.nm) (n=3)	St. Dev - Peak Distribution (d.nm) (n=3)
T - PEG(5k)/DTE-SA	35.5 (0.6)	0.269 (0.021)	34.4 (0.2)/2659 (1209)	10.3 (0.2)/970 (83)
T - PEG(5k)/DTO-SA	33.4 (0.2)	0.056 (0.004)	35.7 (0.1)	9.5 (0.1)
T - PEG(5k)/DTD-SA	33.7 (0.2)	0.061 (0.007)	36.3 (0.1)	9.7 (0.1)
D - PEG(5k)/DTE-SA	188.9 (8.9)	0.222 (0.024)	245.6 (22.9)	134.7 (30.7)
D - PEG(5k)/DTO-SA	143.5 (3.4)	0.126 (0.009)	165.7 (2.8)	63.7 (3.3)
D - PEG(5k)/DTD-SA	174.8 (0.7)	0.136 (0.007)	204.6 (0.6)	79.0 (3.7)

In parenthesis is the standard deviation of the triplicate. All samples met the DLS quality criteria for analysis. T – Triblock, D – Diblock.

The particle sizes of the cholesterol-loaded FNPs were summarize in Table 8. Most of the particle size distributions were bimodal, which was indicative of small populations of unloaded nanoparticles and cholesterol-loading nanoparticles. Nevertheless, the average particle sizes were all small enough to be suitable for intravenous injections and other common drug delivery methods.

Table 8. TyPS-cholesterol FNP hydrodynamic particle diameters

	FNP hydrodynamic diameter (nm) (Z-average) at targeted load levels				
	1%	**3%**	**5%**	**7%**	**10%**
T-DTE-PEG5k	44	42	47	45	43
T-DTO-PEG5k	34	72	95	118	116
T-DTD-PEG5k	34	35	35	48	114
D-DTE-PEG5k	220	203	230	222	207
D-DTO-PEG5k	139	137	99	98	99
D-DTD-PEG5k	171	175	175	183	175

The cholesterol loading levels of the FNPs determined by HPLC were summarized in Figure 7:

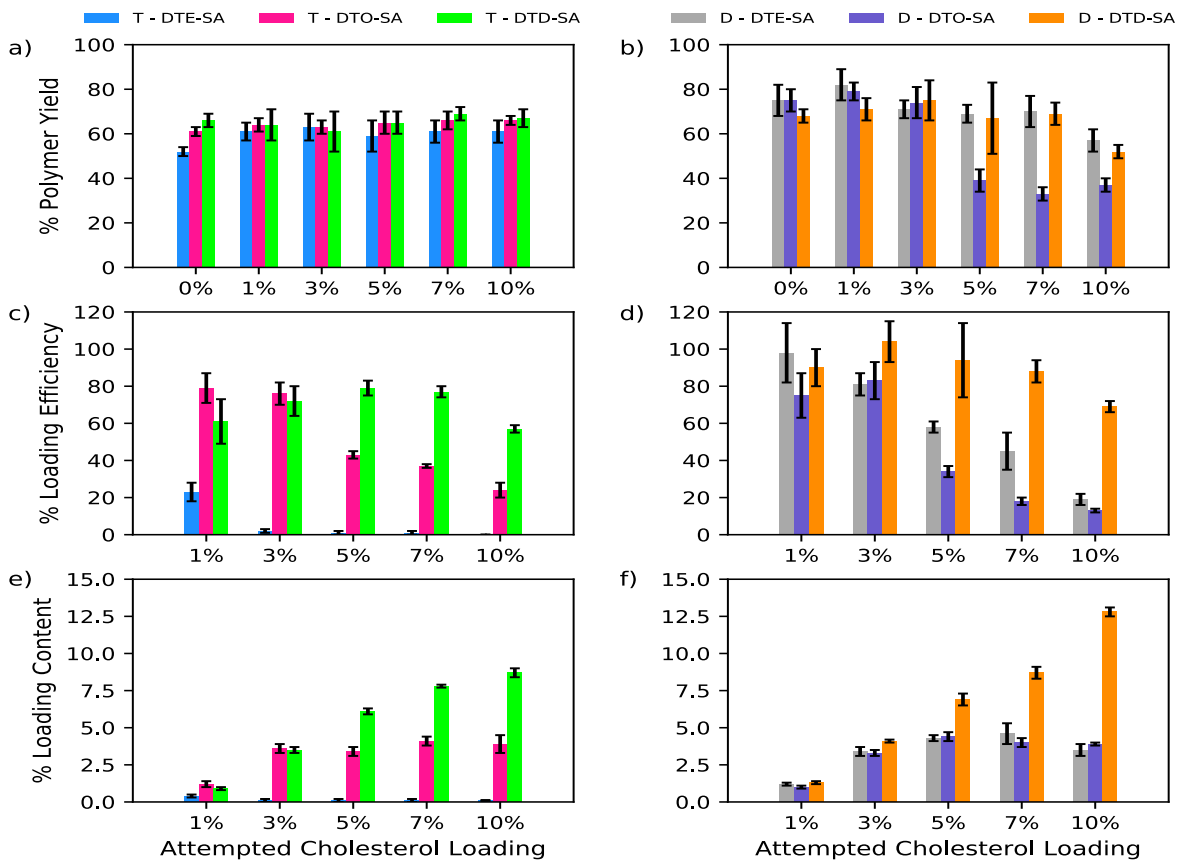

Figure 7. TyPS-cholesterol FNP yield, loading efficiency and loading level. a) % polymer yield of triblock copolymers, b) % polymer yield of diblock copolymers, c) % loading efficiency of triblock copolymers, d) % loading efficiency of diblock copolymers, e) % loading content of triblock copolymers, f) % loading content of diblock copolymers. Triblock copolymers: PEG(5k)/DTE-SA in blue, PEG(5k)/DTO-SA in pink, PEG(5k)/DTD-SA in green. Diblock copolymers: PEG(5k)/DTE-SA in grey, PEG(5k)/DTO-SA in purple, PEG(5k)/DTD-SA in orange.

The FNPs prepared with the diblock D-PEG(5k)/DTD-SA and triblock T-PEG(5k)/DTD-SA were the most effective for attaining high cholesterol loading levels. That result was consistent with the Flory-Huggins interaction parameter values (Table 2).

3.2. Cholesterol controlled release kinetics from the FNPs. Despite the extremely low solubility of cholesterol in aqueous solution, 9.5×10^{-5} mg/mL, a linear calibration curve was obtained using high performance liquid chromatography (HPLC) and the release of cholesterol from the functional nanoparticle (FNP) comprised of triblock TyPS T-DTD and 5% cholesterol (Figure 8) was obtained by equilibrium membrane dialysis in PBS. Although there was significant variation in individual time points, the release appeared typical of FNP release of other hydrophobic drugs with a rapid early stage followed by a slower stage.

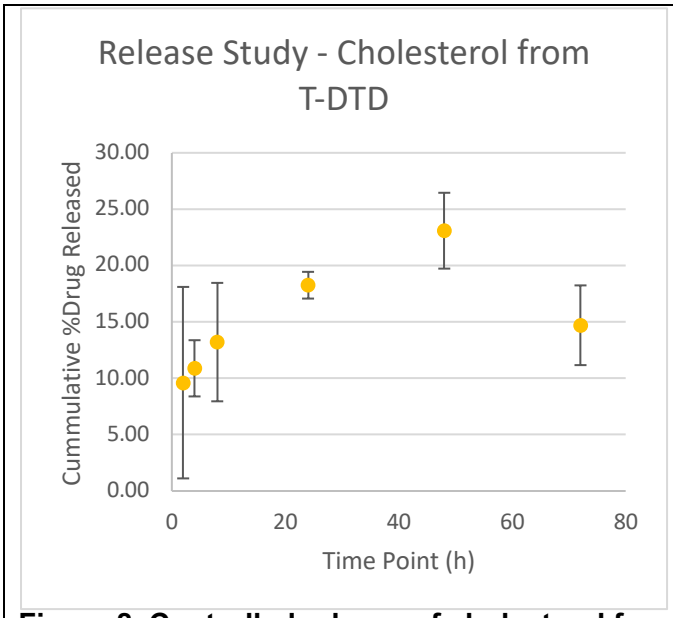

Figure 8. Controlled release of cholesterol from an FNP of T-DTD/5%cholesterol

3.3. Partition coefficients, $log_{10}P(o/w)$ for the FNPs. Method development for determination of the partition coefficients for the TyPS-cholesterol FNPs was initiated [26] and those studies will be completed in the first quarter of 2021.

Task 4. IACUC and ACURO animal protocol reviews

4.1. Document rat tibial nerve protocol and submit to Rutgers IACUC and US Army ACURO. The rat nerve injury protocol which we will use to evaluate the in vivo fusogenic efficacy of TyPS-cholesterol FNPs was submitted first to the Rutgers Institutional Animal Care and Use Committee (IACUC) and, following their approval, it was submitted to the US Army Animal Use and Care Review Office (ACURO), which gave its approval to the protocol on March 19, 2020. The formal triennial revue required by Rutgers University on this recurrent protocol will take place in January, 2021. Because of its recent approval by the Rutgers IACUC, no issues are foreseen. Briefly, in the protocol the rat tibial nerve will be isolated, surgically transected, immediately repaired with microsutures to reproduce the axonal overlapping routinely achieved in standard end-to-end nerve coaptation in clinical practice, treated with the fusogens and characterized using electrophysiological and histological measurements.

Specific Aim 2: Evaluation of functional nanoparticle (FNP) *in vitro* axonal membrane repair and cytotoxicity

Task 5: FNP repair of dorsal root ganglion (DRG) axon membranes.

5.1: Compare the efficacy of FNPs, PEG and P188 for fusion of severed DRG axon fusion based on fluorochrome dynamics. In this in vitro study we aimed to demonstrate axonal fusion using rat dorsal root ganglions (DRGs). 3D-printed polycaprolactone (PCL) scaffolds were employed in the experiments for cell seeding and as guidance templates for surgical blade-cut transection of single axons. A published single-axon mechanical blade-cut method has been reported which required the use of a custom-made manufactured micro-blade.[27] We focused instead on using commercially available surgical blades which are routinely used in peripheral

nerve surgery by developing a 3D printed scaffold that enabled the positioning and holding of the blade. The printed scaffold design enabled visualization of axonal growth, transection and fusion. The PCL scaffolds were printed using an EnvisionTec 3D Bioplotter (Manufacturer Series, Inc., Deaborn, MI). Scaffold models were designed in Sketchup (Google, Inc., Mountain View, CA), exported as STL files and translated into printable g-code files using Perfactory Rapid Prototype (RP) (EnvisionTEC, Inc., Dearborn, MI). The scaffolds provided two separate compartments for DRGs stained with either red or green fluorescent dyes to grow and intersect, two compartments for growth media exchange, and a guidance channel compartment to enable precise surgical blade cuts of single axons. The overall wall thickness of the scaffold was 0.1mm and the height was 3 mm. The scaffolds rested on a glass surface and were sealed to the surface with polydimethylsulfoxide (PDMS). Scaffolds were washed with Ultrapure sterile water and sterilized under UV for 1h. The scaffolds were coated with 20µg/mL poly(ethylene imine) (PEI) in PBS to promote DRG adhesion.

In addition to the novel 3D scaffold design and fabrication, methods had to be developed for: 1) in vitro culture of rat embryo DRGs to obtain a significant growth of axons (neurites) at least 1 mm in length; 2) a practical and reproducible technique for the mechanical blade-cut of single axons; and, 3) a low-cost technique to differentially stain the DRGs with red and green vital fluorochromes markers which did not affect cell viability. Rat DRGs were kindly provided in a hibernating media by Robert Shultz, PhD, from the University of Pennsylvania. One DRG was seeded to each compartment of the scaffold with the aid of 200µL pipette tip. Then, DRG Complete media containing neurobasal (ThermoFisher 21103049), 2.5 g/L Glucose (Sigma G7528), 1% v/v FBS (Atlanta Biologicals S11195), 0.25% v/v Glutamax (ThermoFisher 35050061), 20 ng/mL NGF (Sigma N6009), 40 uM 5FDU (Sigma F0503), 40 uM 5FDU (Sigma F0503), 40 uM Uridine (Sigma U6381), 1x B-27 (ThermoFisher 12587010; 2% v/v), and 1% v/v Pen/Strep (ThermoFisher 15140122) was added to the scaffolds and to the other compartments. Samples were incubated in a CO_2 incubator at 37ºC. The DRG in one compartment was stained with fluorescent dye CellTracker Green (5µM in DMSO, CMFDA C2925 Thermofisher) and the DRG in the opposite compartment was stained with fluorescent dye CellTracker Red (CMTPX ThermoFisher). It was anticipated that as the red and green labeled axons grew toward each other, their combination would produce a yellow fluorescent signal which would be univocal indicator of anatomical fusion.

We found that the DRGs could be cultured in the 3D scaffolds and grew to provide axonal lengths up to 3 mm (Figure 9).

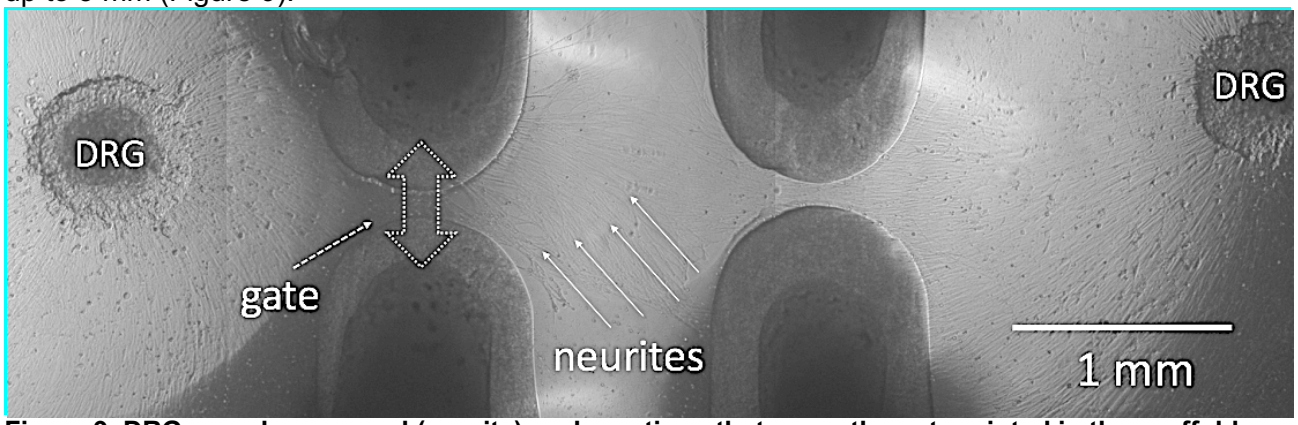

Figure 9. DRG grow long axonal (neurite) prolongations that cross the gate printed in the scaffold and reach the area of mechanical blade cutting.

The 3D-printed scaffolds allowed the precise positioning of a standard #15 surgical blade. Cuts at

the single-axon level were performed multiple times in a reproducible way (Figure 10). The gap produced by the cuts were as short as 4 microns. Following the cuts, however, every gap had the tendency to widen [27] and no overlapping of axons was ever observed following these sharp blade cuts.

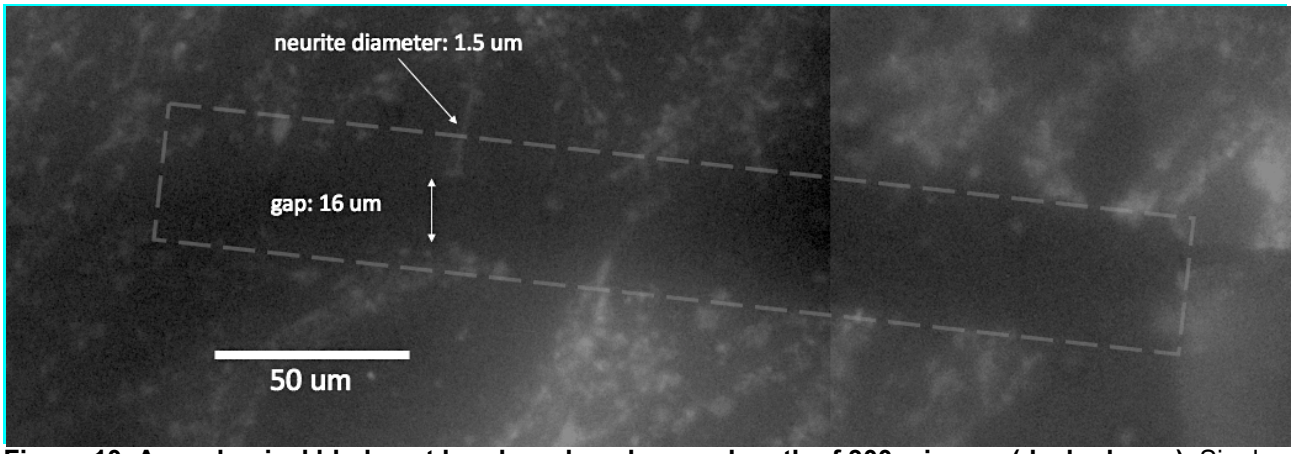

Figure 10. A mechanical blade-cut hand produced over a length of 300 microns (dashed area). Single axonal (neurite) stumps are clearly identified by their morphology and dimensions.

Differential staining of DRGs in the 3D printed scaffold with either red or green CellTracker fluorescent dyes was successful (Figure 11). However, the rapid decrease in fluorescent signals precluded the possibility of confirming fusion through the appearance of a yellow fluorescent signal. More effective fluorescent staining methods are now under consideration.

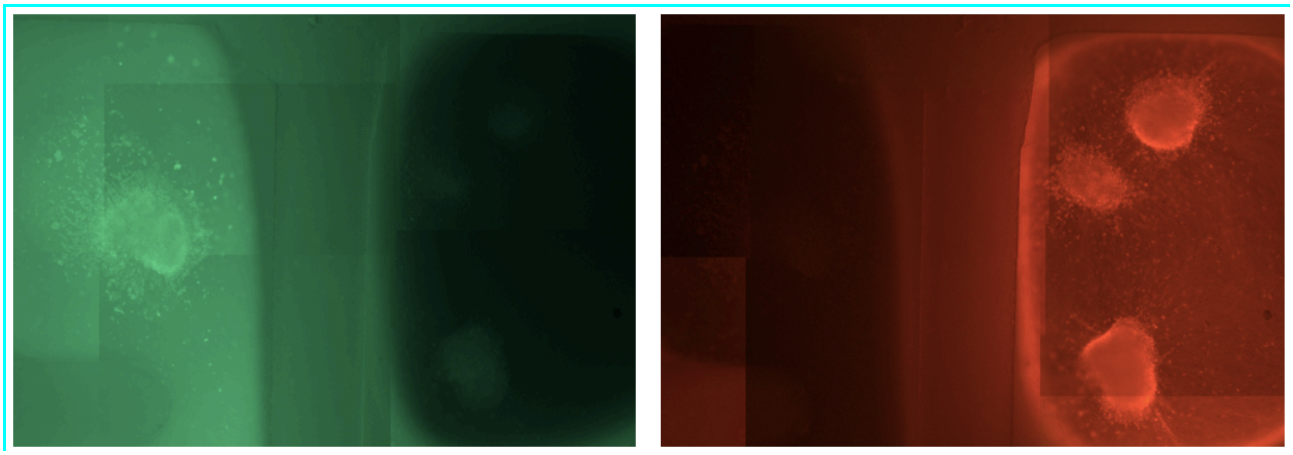

Figure 11. In the same field of view, a green filter shows a green-labeled DRG in the compartment on the left and a red filter shows three red-labeled DRGs in the compartment on the right. Minimal autofluorescence is present in both cases.

Having obtained at least a practical and reproducible method for blade-cuts of DRG axons, a preliminary investigation of the response to the on-site administration of fusogens molecules was initiated using bright-field phase-contrast microscopy and fluorescence microscopy. We used a single DRG compartment scaffold with only one gate and applied 10µl of fusogen solution after cutting. Experiments were performed in triplicate. The fusogens tested were PEG and the functional nanoparticle (FNP) comprised of T-DTD/5%cholesterol. In the control experiment, cut axons again exhibited the tendency to retract. We documented only one episode of axonal stumps overlapping and apparently spontaneously fusing end-to-end (Figure 12). In this single case, when

the field was re-imaged seven hours later the apparent spontaneous fusion was no longer present (Figure 12). Un-cut axons did not change their morphology over a period of 7 days, but then gradually degenerated and broke-up into granules.

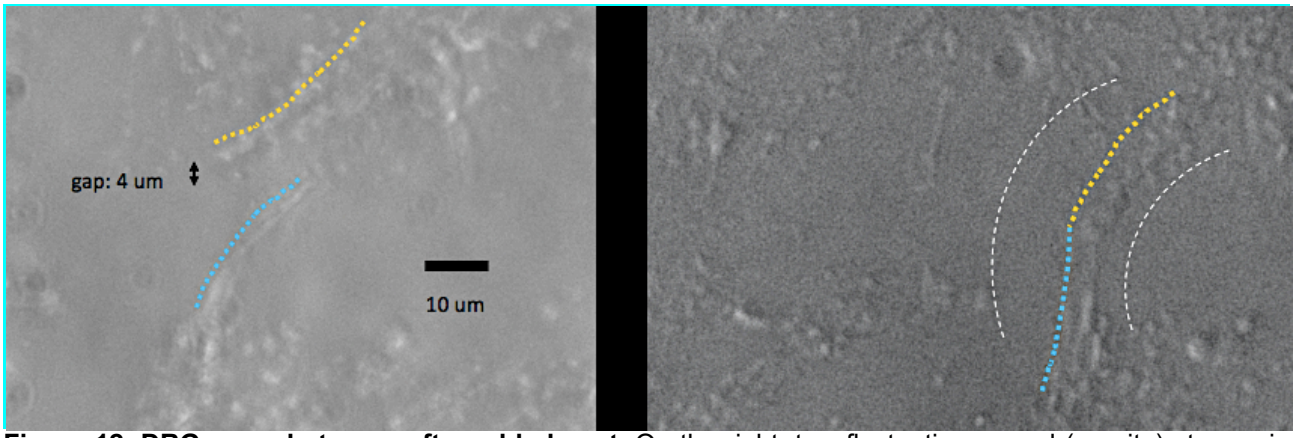

Figure 12. DRG axonal stumps after a blade cut. On the right, two fluctuating axonal (neurite) stumps in the middle of the cut of Figure 11 overlapped and apparently fused end-to-end after 15 minutes. The apparent fusion was documented for 45 minutes but was no longer present after a new imaging at 7 hours.

Application of 50% PEG solution did not prevent cut axons from retracting. However, PEG did change the morphology of the branching axons and imaging was suggestive of some side-by-side axonal fusion (Figures 13 and 14). A mechanism of side-by-side fusion could explain the immediate re-establishment of signal conduction and the reduced or absent Wallerian degeneration which has been reported in the literature about PEG-induced nerve repair.[28]

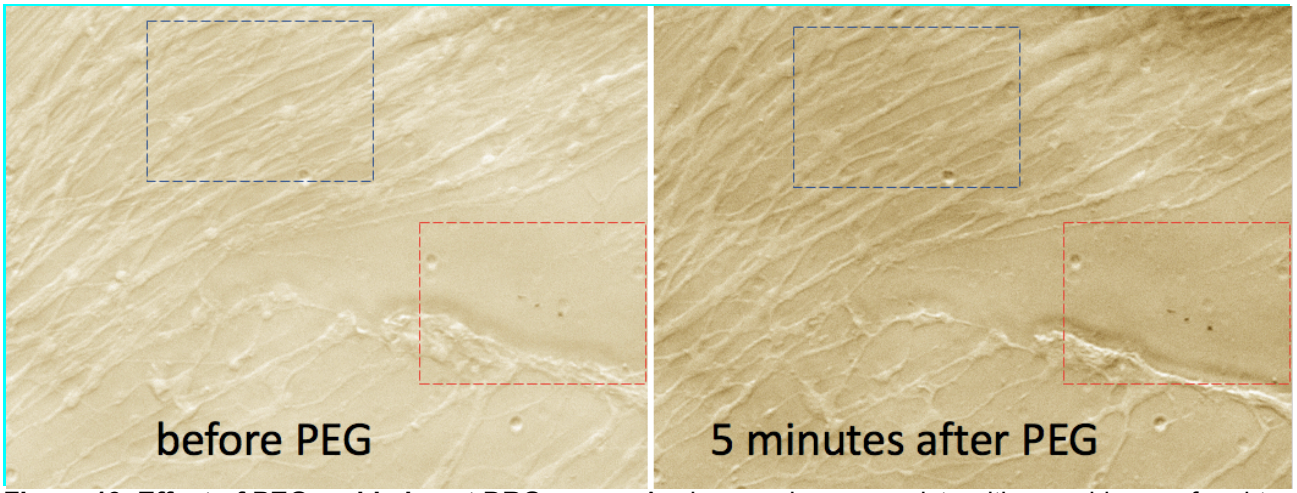

Figure 13. Effect of PEG on blade-cut DRG axons. A microscopic gap persists with no evidence of end-to-end fusion after PEG administration (red square). Close to the cut, changes in axonal (neurite) morphology and images suggestive of side-by-side fusion appear (blue square).

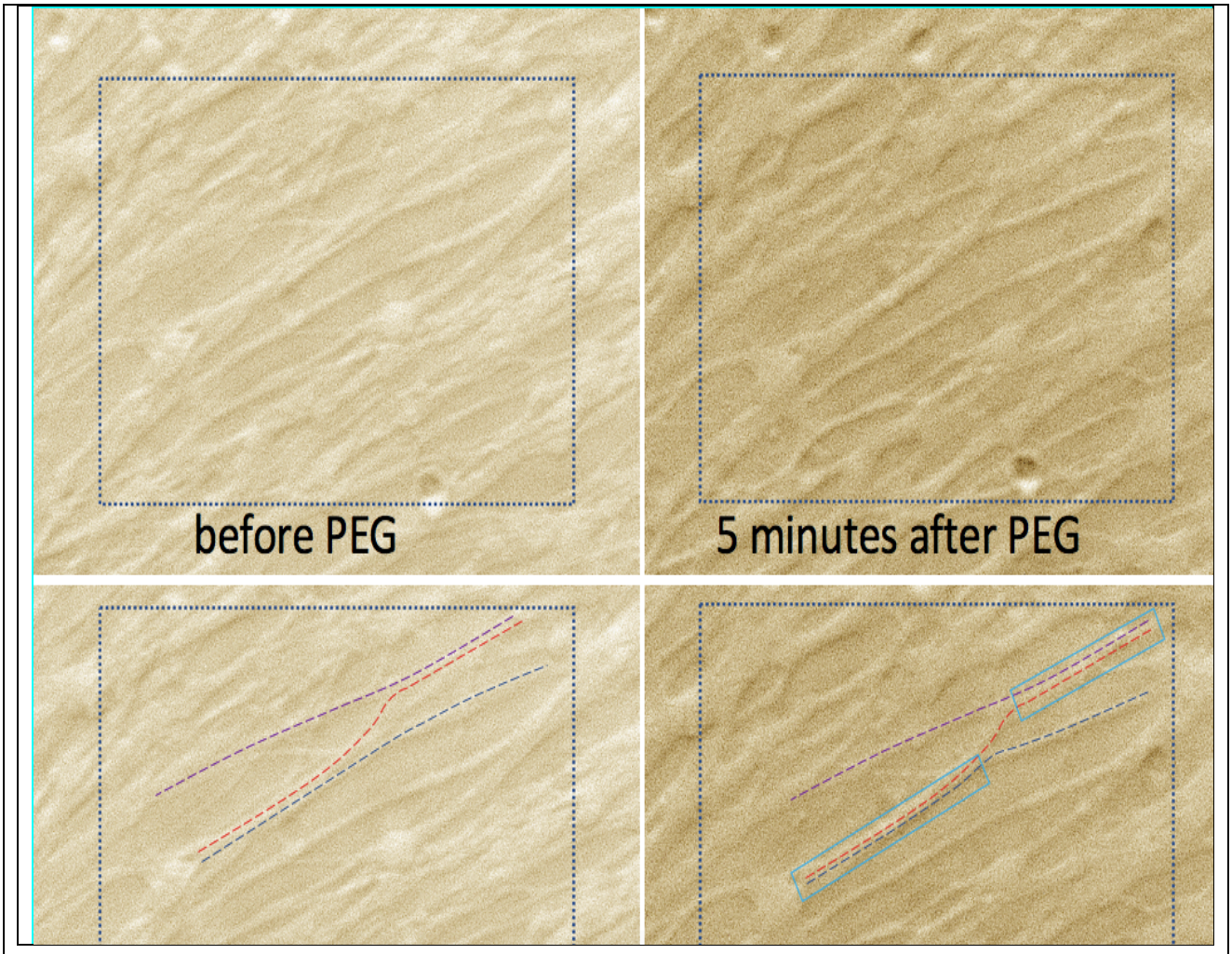

Figure 14. Detail from Figure 13. 3 axons (neurites) are traced that appear to show regions of side-by-side fusion (light blue solid squares).

Similar to the results with PEG, the FNP of T-DTSD/5%cholesterol did not prevent retraction of the cut axon ends and no evidence of end-to-end axonal fusion was observed. Unlike with PEG treatment, the branching of axons was not modified by the FNP and they remained intact but, unlike with PEG, no images suggestive of side-by-side axonal fusion was observed. The DRG studies will be pursued in Year 2 to fully evaluate the effects of PEG, P188, selected TyPSs and FNPs.

5.2: Determine the efficacy of Fusogen Nanoparticles (FNPs) for delivery of cholesterol to DRG axonal membranes based on quantitative HPLC analysis. Per the project Statement of Work, these studies are planned for Year 2 and are anticipated to commence in February, 2021.

Task 6. Cytotoxicity of Fusogen Nanoparticles (FNPs).

6.1. Determine the cytotoxicity of FNPs, TyPSs, PEG and P188 based on viability assays for human endothelial cells and primary nerve cells. Human dermal microvascular endothelial cells (HDMEC) were purchased from ScienCell (Cat#2000 Lot# 4019). Endothelial cell growth medium kit containing Growth medium base (C-22010B Lot# 1x456M141) and SupplementMix (C-

39215 Lot# 1x452M171) was purchased from PromoCell. Cells (passage 3) were thawed and cultured in endothelial cell growth medium at 37°C with 5% CO_2 and 95% humidity following manufacture's instruction. HDMEC cells were seeded at $2x10^4$/well in 96-well plates in endothelial cell growth medium. After incubation at 37°C for 24 h, media were removed from each well. 100 µL medium with or without serially diluted concentrations of diblock and triblock TyPS was added to each designated well. Cells were incubated at 37°C for 24 h. After incubation, medium was removed from each well and cells were washed with phosphate buffered saline (PBS) two times. 100 µL of medium containing 10% alamarBlue reagent (Bio-Rad Cat# BUF012A) was added to each well. After incubation at 37°C for 1h, the fluorescence intensity was measured using TECAN Spark plate reader at Ex540nm/Em590nm.

The viability of the HDMECs in the presence of TyPS was normalized to that of untreated HDMECs and, as shown in Figure 15, the HDMECs maintained between 100% and 80% viability even at the high dosage of 10% TyPS solutions. Based on the criteria in ISO Standard 10993-5, it was concluded that none of the TyPS were cytotoxic to HDMEC. That result was consistent with our previous studies with similar TyPS compositions.

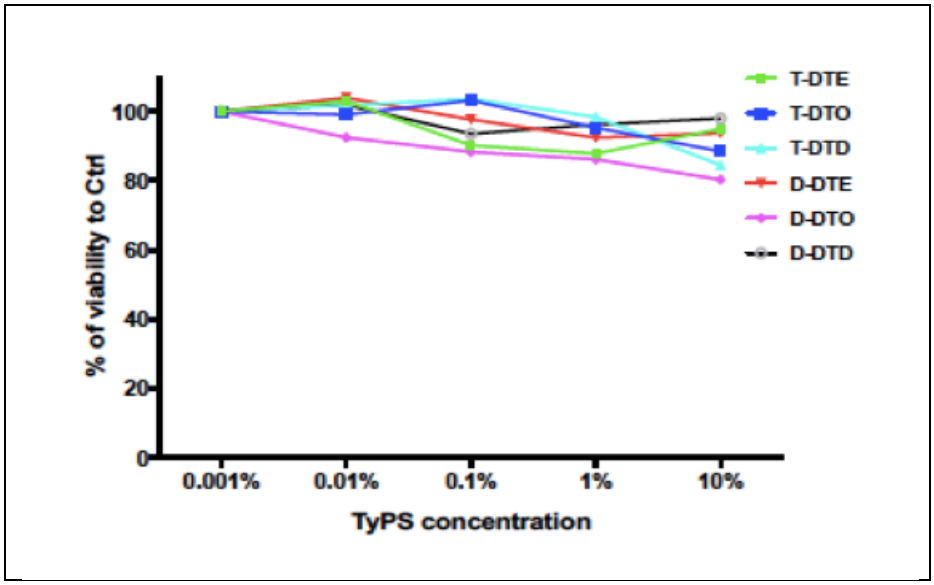

Figure 15. Viability of human dermal microvascular cells in the presence of increasing concentrations of diblock and triblock TyPS. PEG(5kDa) used in all of these TyPS.

The diblock and triblock TyPS were then formulated into Fusogen Nanoparticles (FNPs) using the procedure described in section 3.1 above and their cytotoxicities to HDMECs was determined using the alamarBlue viability assay. The amount of cholesterol incorporated in these FNPs was chosen to assure that the FNPs were stable at room temperature for several days. PEG was also tested in these experiments and it was noted that 50% wt:vol concentration was the concentration which had been shown to be effective for the fusion of nerves and other cells.[29] Remarkably, the viability of the HDMECs was increased by all of the FNPs and at the highest tested concentration of 10% FNP, the triblocks were particularly effective at increasing the cell viability whereas the PEG actually demonstrated some cytotoxicity at that high 10% concentration (i.e., at a lower concentration than the 50% which is used in PEG cell fusion applications) (Figure 16).

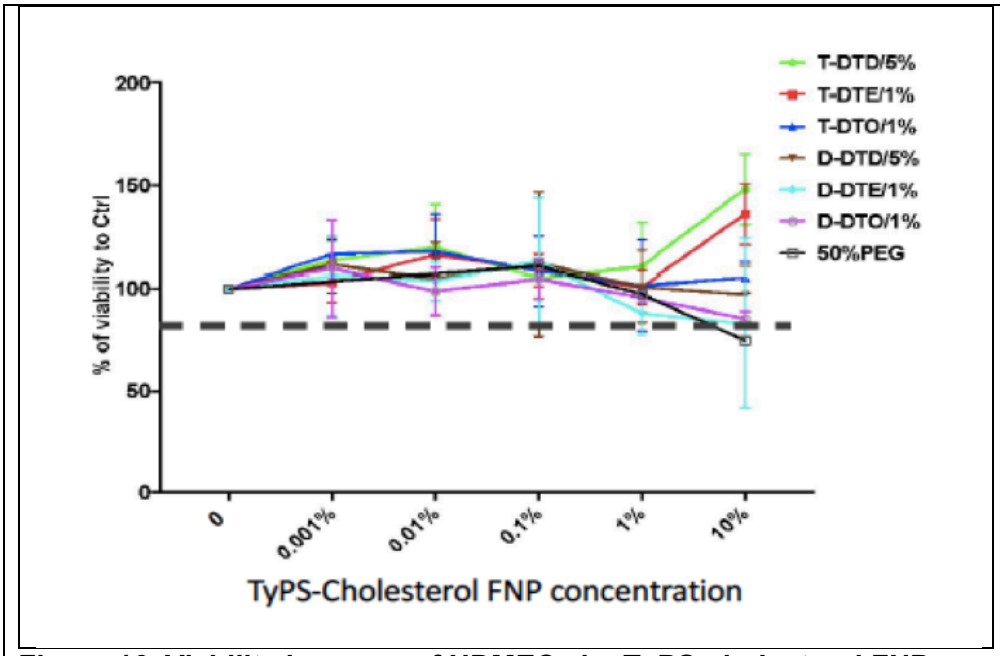

Figure 16. Viability increase of HDMECs by TyPS-cholesterol FNPs

Neuronal cell viability and fusion were determined by flow cytometry with B35 rat neuroblastoma cells treated with PEG, P188 and the diblock and triblock TyPSs. Flow cytometry was not specifically included in the original project plan but was considered to offer potentially important insights into the cytotoxicity and fusogenic activity of the fusogens which cannot be as readily determined by other methods. It remains to be seen if the cell membrane processes observed with flow cytometry in this neural cell line are conserved in axonal fusion. This flow cytometry work was not carried out nor paid for by the Fusogen Nanomedicine project. Rather, it was another project at Rutgers conducted under a separate NIH T-32 fellowship project which had relevant information for this project and the results are cited here. The method used here initially followed a published approach which had been used to demonstrate the fusion of rat B35 neuroblastoma cells by 50% PEG solution.[30] In that published approach, the neuroblastoma cells were labelled using CellTracker Green and CellTracker Violet fluorescent dyes. The amount of fusion was measured as the number of double positive cells in the flow cytometer. The PEG exposure time was 1 min, followed by a wash-out and then the number of fused cells was determined. Cell viability was then measured using propidium iodide. It was reported that as PEG concentration was increased from 10% to 100%, cell fusion increased from 2% to 10% of the cell population but cell viability decreased from 96% to 83%. That observation was consistent with other reports of the cytotoxicity of high PEG concentrations on other cell types.

We were able to reproduce those published results for PEG and demonstrated that PEG was statistically far superior to the diblock TyPS while the triblock TyPS and P188 were relatively ineffective (table 9). Given that the TyPS had no cytotoxicity in the HDMEC viability assays, we made a modification in the flow cytometry protocol: exposure time to the fusogens was increased to 2hr, and in a separate experiment, to 24hr. A typical set of results obtained at the 24hr time point was illustrated in Figure 17. Those longer exposures were justified on the basis of the lower dosages and slower diffusion of the high molecular TyPS relative to PEG, as well as the planned in vivo nerve transection experiments to be performed in Year 2, in which the fusogens will be injected at the surgical transection site and hence could be present in appreciable concentration for several hours.

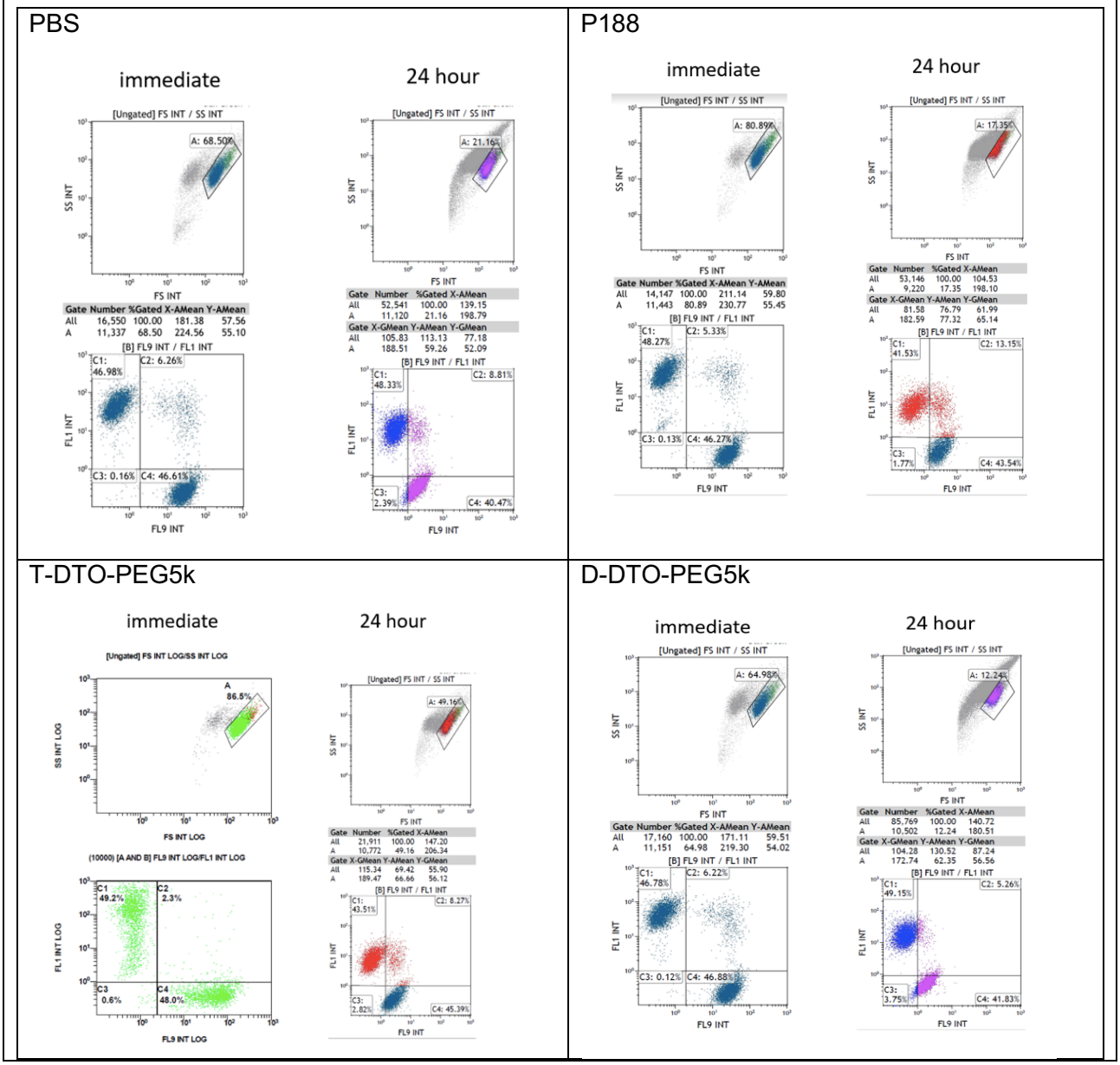

Figure 17. Flow cytometry of rat B35 neuroblastoma cells exposed to PBS (control), P188, and diblock and triblock TyPSs.

The flow cytometry experiments were repeated in triplicates and analysis of variance (ANOVA) for each time point was performed. The results of the flow cytometry experiments were summarized in Table 9.

Table 9. Flow cytometry of neuroblastoma cells treated with PEG, P188, TyPSs and FNPs

Treatment	Dosage (mg/mL)	Exposure Time	Whole Cell Viability (%)	Fused Cells (%)
PBS	-	1 min	81.8+/-18.7	5.5 +/-1.2
PBS	-	2 hr	49.0+/-8.8	0.65+/-0.07
PBS	-	24 hr	27.7+/-9.5	8.3+/-1.4
PEG	500	1 min	79.8+/-4.2	11.3+/-1.0
PEG	500	2 hr	0	0
PEG	500	24 hr	-	-
P188	40	1 min	81.3+/-0.4	4.7+/-0.5
P188	40	2 hr	75.2+/-0.6	4.0+/-0.2
P188	40	24 hr	18.6+/-3.4	11.9+/-1.4
T-DTD	40	1 min	90.4+/-5.8	2.9+/-0.6
T-DTD	40	2 hr	76.2+/-1.7	4.1+/-0.2
T-DTD	40	24 hr	49.2+/-2.8	7.6+/-0.8
FNP T-DTD/Cholesterol 5%	40	1min	63.3+/-3.8	3.4+/-0.2
FNP T-DTD/Cholesterol 5%	40	2 hr	77.7+/-1.9	4.3+/-0.3
T-DTO	40	1 min	83.1+/-4.6	2.7+/-0.4
T-DTO	40	2 hr	72.3+/-2.9	2.3+/-0.3
T-DTO	40	24 hr	50.6+/-5.4	7.9+/-0.4
FNP T-DTO/Cholesterol 1%	40	1min	47.1+/-23.3	2.6+/-2.2
FNP T-DTO/Cholesterol 1%	40	2 hr	75.9+/-3.3	3.8+/-0.4
T-DTE	40	1 min	83.2+/-2.9	1.9+/-0.1
T-DTE	40	2 hr	75.6+/-0.6	2.7+/-0.1
T-DTE	40	24 hr	49.0+/-6.8	8.2+/-0.6
FNP T-TDE/Cholesterol 1%	40	1min	62.0+/-2.6	4.6+/-0.2
FNP T-TDE/Cholesterol 1%	40	2 hr	78.6+/-0.8	3.0+/-0.2
D-DTD	40	1 min	65.1+/-4.0	6.7+/-0.6
D-DTD	40	2 hr	tbd	tbd
D-DTD	40	24 hr	14.0+/-0.8	5.8+/-0.9
D-DTO	40	1 min	67.2+/-2.6	6.7+/-0.5
D-DTO	40	2 hr	tbd	tbd
D-DTO	40	24 hr	12.7+/-2.7	6.4+/-1.2
D-DTE	40	1 min	38.0+/-5.8	4.8+/-0.5
D-DTE	40	2 hr	tbd	tbd
D-DTE	40	24 hr	20.8+/-2.3	6.4+/-0.5

After 2 hr exposure time, the viability of the neuroblastoma cells decreased to zero for PEG and

approximately 20% for the PBS control, P188 and the diblock TyPS, but the triblock TyPSs provided superior survival with 40-50% viability. In addition, the number of fused cells was greater in the presence of the triblock TyPS and P188 than with the diblock TyPS, PEG or PBS (Figure 15) Similar trends in fusogenic behavior were observed after 2hr exposure times, while the viability of the cells was far greater at 2hr than 24hr for all treatments. Although flow cytometry for a few time points remain to be completed, it was concluded that the TyPS provided greater cell viability and fusion over time than PEG, which was cytotoxic at long exposure times. These observations will be used to guide the time course and dosage levels of the fusogens to be applied in the Year 2 in vivo rat tibial nerve transection experiments.

6.2. Determine the hemolytic activity of FNPs, TyPS, PEG and P188. A protocol for determining the effects of the fusogens on human red blood cells was developed and approved by Rutgers IACUC. The protocol requires collection of human blood samples from volunteers. The protocol will be implemented in Year 2 pending approval from the US Army Human Research Protection Office.

Specific Aim 3:Evaluation of the lead FNP in an in vivo rat tibial nerve injury model.
Per the project Statement of Work, these in vivo studies were planned for Year 2. The ACURO protocol has been approved and work will commence by May, 2021.

REFERENCES

1. Nardin C, Bolikal D, Kohn J, Nontoxic Block Copolymer Nanospheres: Design and Characterization. *Langmuir*. 2004;20(26):11721-11725. doi:10.1021/la0490285
2. Sheihet L, Dubin RA, Devore D, Kohn J, Hydrophobic Drug Delivery by Self-Assembling Triblock Copolymer-Derived Nanospheres. *Biomacromolecules*. 2005;6(5):2726-2731. doi:10.1021/bm050212u
3. Lima M, Le K-P, Kohn J, Devore D, Thermodynamic properties of tyrosine-derived diblock and triblock polymeric surfactants, manuscript in preparation.
4. Aydin F, Chu X, Uppaladadium G, Devore D, Goyal R, Murthy NS, Zhang Z, Kohn J, Dutt Meenakshi, Self-Assembly and Critical Aggregation Concentration Measurements of ABA Triblock Copolymers with Varying B Block Types: Model Development, Prediction, and Validation. *The journal of physical chemistry B*. 2016;120(15):3666-3676. doi:10.1021/acs.jpcb.5b12594
5. Sheihet L, Piotrowska K, Dubin RA, Kohn J, Devore D, Effect of Tyrosine-Derived Triblock Copolymer Compositions on Nanosphere Self-Assembly and Drug Delivery. *Biomacromolecules*. 2007;8(3):998-1003. doi:10.1021/bm060860t
6. Sheihet L. Garbuzenko OB, Bushman J, Gounder MK, Minko T, Kohn J, Paclitaxel in tyrosine-derived nanospheres as a potential anti-cancer agent: In vivo evaluation of toxicity and efficacy in comparison with paclitaxel in Cremophor. *European journal of pharmaceutical sciences*. 2012;45(3):320-329. doi:10.1016/j.ejps.2011.11.017
7. Thakral S, Thakral NK. Prediction of Drug–Polymer Miscibility through the use of Solubility Parameter based Flory–Huggins Interaction Parameter and the Experimental Validation: PEG as Model Polymer. *Journal of Pharmaceutical Sciences*. 2013;102(7):2254-2263. doi:10.1002/jps.23583
8. Krevelen, D.W. van, and Klaas te Nijenhuis. Properties of Polymers: Their Correlation with Chemical Structure; Their Numerical Estimation and Prediction from Additive Group

Contributions, Elsevier Science & Technology, 2009.
9. Grulke EA, Solubility Parameter Values, in Polymer Handbook, 3rd ed., Brandrup J, Immergut EH, eds., Wiley, New York, 1989.
10. Barton A. Applications of solubility parameters and other cohesion parameters in polymer science and technology. *Pure and Applied Chemistry Chimie Pure et Appliquee*. 1985;57(7):905-912. doi:10.1351/pac198557070905
11. David D., Sincock T. Estimation of miscibility of polymer blends using the solubility parameter concept. *Polymer*. 1992;33(21):4505-4514. doi:10.1016/0032-3861(92)90406-M
12. Liron Z, Cohen S, Densitometric determination of the solubility parameter and molal volume of compounds of medicinal relevance, *Journal of Pharmaceutical Sciences* 1983; 72:499-504. https://doi.org/10.1002/jps.2600720506
13. Özdemir C, Güner A. Solubility profiles of poly(ethylene glycol)/solvent systems, I: Qualitative comparison of solubility parameter approaches. *European Polymer Journal*. 2007;43(7):3068-3093. doi:10.1016/j.eurpolymj.2007.02.022
14. Mieczkowski R. Solubility parameter components of some polyols. *European Polymer Journal*. 1991;27(4-5):377-379. doi:10.1016/0014-3057(91)90191-P
15. Davies JT, Rideal EK. *Interfacial Phenomena*. 2nd ed. Academic Press; 1963, pp.371-383.
16. Morrison ID, Ross S, Colloidal Dispersions, Wiley, New York, 2002, pp.429-432.
17. Lin IJ, Friend JP, Zimmels Y, The effect of structural modifications on the hydrophile—lipophile balance of ionic surfactants. *Journal of Colloid and Interface Science*. 1973;45(2):378-85.
18. Guo X, Rong Z, Ying X. Calculation of hydrophile–lipophile balance for polyethoxylated surfactants by group contribution method. *Journal of Colloid and Interface Science*. 2006;298(1):441-450. doi:10.1016/j.jcis.2005.12.009.
19. Kabanov AV, Nazarova IR, Astafieva IV, et al. Micelle Formation and Solubilization of Fluorescent Probes in Poly(oxyethylene-b-oxypropylene-b-oxyethylene) Solutions. *Macromolecules*. 1995;28(7):2303-2314. doi:10.1021/ma00111a026.
20. Nagarajan R, Ganesh K, Comparison of Solubilization of Hydrocarbons in (PEO–PPO) Diblock versus (PEO–PPO–PEO) Triblock Copolymer Micelles. *Journal of colloid and interface science*. 1996;184(2):489-499. doi:10.1006/jcis.1996.0644.
21. Scholz N, Behnke T, Resch-Genger U, Determination of the Critical Micelle Concentration of Neutral and Ionic Surfactants with Fluorometry, Conductometry, and Surface Tension—A Method Comparison. *Journal of fluorescence*. 2018;28(1):465-476. doi:10.1007/s10895-018-2209-4.
22. Batrakova E, Lee S, Li S, Venne A, Alakhov V, Kabanov A,Fundamental Relationships Between the Composition of Pluronic Block Copolymers and Their Hypersensitization Effect in MDR Cancer Cells. *Pharmaceutical research*. 1999;16(9):1373-1379. doi:10.1023/A:1018942823676.
23. Maskarinec S, Hannig J, Lee RC, Lee K, Yee C, Direct Observation of Poloxamer 188 Insertion into Lipid Monolayers. *Biophysical journal*. 2002;82(3):1453-1459. doi:10.1016/s0006-3495(02)75499-4.
24. Prescher H, Ling M, Lee RC, Copolymer Surfactant Poloxamer 188 Accelerates Post-axonotemetic Sciatic Nerve Regeneration. *Regenerative Engineering and Translational Medicine.* 2020. https://doi.org/10.1007/s40883-020-00174-y.
25. Ottico E, Prinetti A, Prioni S, Giannotta C, Basso L, Chigorno V, Sonnino S, Dynamics of membrane lipid domains in neuronal cells differentiated in culture. *Journal of lipid research*. 2003;44(11):2142-2151. doi:10.1194/jlr.m300247-jlr200.
26. Sangster J, Octanol-water partition coefficients for simple organic compounds. *Journal of Physical and Chemical Reference Data*. 1989;18, 1111-1226. https://doi.org/10.1063/1.555833
27. Chang WC, Hawkes E, Keller CG, Sretavan DW, Axon repair: surgical application at a

subcellular scale. *WIREs Nanomed Nanobiotechnol* 2010; 2: 151–161. doi:10.1002/wnan.76.
28. Giordano-Santini R, Linton C, Hilliard MA, Cell-cell fusion in the nervous system: Alternative mechanisms of development, injury, and repair. *Seminars in cell & developmental biology*. 2016;60:146-154. doi:10.1016/j.semcdb.2016.06.019
29. Bittner GD, Cameron MM, Ghergherehchi L, Polyethylene glycol-fusion retards Wallerian degeneration and rapidly restores behaviors lost after nerve severance. *Neural regeneration research*. 2016;11(2):217-219. doi:10.4103/1673-5374.177716.
30. Hoffman A, Bamba R, Pollins A, Thayer WP, Analysis of polyethylene glycol (PEG) fusion in cultured neuroblastoma cells via flow cytometry: Techniques & optimization. *Journal of clinical neuroscience*. 2017;36:125-128. doi:10.1016/j.jocn.2016.10.032.

What opportunities for training and professional development has the project provided?

Mariana Lima is a graduate student in the Department of Chemistry and Chemical Biology at Rutgers University. Her thesis work on this project has been guided by Prof. Joachim Kohn and Dr. David Devore. Mariana anticipates graduating with a Doctorate in Chemistry in June, 2021.

Daniel Chakhalian, MD, is an NIH T-32 Postdoctoral Fellow who has been mentored by Prof. Joachim Kohn and Prof. Kacy Cullen at the University of Pennsylvania. Dr. Chakhalian is on leave from clinical programs for the purpose of professional development as a medical research scientist and physician.

Cemile Bektas, PhD, is an NIH T-32 Postdoctoral Associate who has been mentored by Prof. Joachim Kohn and Prof. Kibum Lee in the Department of Chemistry and Chemical Biology at Rutgers University. She has contributed to this work through 3D printing of the DRG scaffolds and in vitro studies. She will be contributing to in vivo studies

How were the results disseminated to communities of interest?

Dr. Devore, Dr. Chakhalian and Mariana Lima provided seminars on their research efforts under this project to the New Jersey Center for Biomaterials research group, which includes undergraduate students, graduate students, postdoctoral fellows and research faculty members.

What do you plan to do during the next reporting period to accomplish the goals?

In the first half of Year 2, we will complete the hemolysis and dorsal root ganglia (DRG) studies. If the hemolysis and DRG results align with the Langmuir film data and the human dermal cell and rat neuroblastoma cytotoxicity data, we will select the candidate TyPS-based functional nanoparticle (FPN) to start the in vivo rat tibial nerve transection experiments. If none of the first set of TyPS FNPs, with or without cholesterol, appear to provide a satisfactory combination of properties including low cytotoxicity, low hemolysis, high cell viability and high fusogenic activity, then we will synthesize and characterize in vitro a second, narrowly focused set of additional TyPS which may produce an improved combination of low cytoxocity, low hemolysis, high cell viability and high cell fusion activity. While this iterative approach may take a few months, we are close to the project timeline in the Statement of Work and expect to complete all Tasks on time.

4. IMPACT:

What was the impact on the development of the principal discipline(s) of the project?

We are preparing manuscripts for publication which we anticipate will have a significant impact on the field, particularly if we can demonstrate that the TyPS FNPs provide improved fusion of transected nerves and that side-by-side axonal fusion is a frequent and reproducible result of fusogen treatments.

What was the impact on other disciplines?

Nothing to report.

What was the impact on technology transfer?

An Invention Disclosure has been submitted by Dr. David Devore and Prof. Joachim Kohn to Rutgers Innovation Ventures group for review. The disclosure covers compositions of matter and methods of use of the diverse polymeric surfactants such as the TyPS for cell surface modification including nerve fusion. It is anticipated that a Provisional Patent based on this Invention Disclosure will be filed in the first quarter of 2021.

What was the impact on society beyond science and technology?

Nothing to report.

5. CHANGES/PROBLEMS:

Rutgers, The State University of New Jersey ("Rutgers") will be submitting for review/approval per our Contract Terms and Conditions as delineated in the DoD Research General Award Terms and Conditions, FMS Article IV. a respectful request for a change of Principal Investigator from Dr. Joachim Kohn to Dr. Wise Young. This request is respectfully put forth as Dr Kohn retired from Rutgers with an effective date of November 1, 2020. Dr. Young was asked to assume the role of Principal Investigator of the Fusogen project due to his extensive experience and interest in the topic. Dr. Wise Young has been conducting spinal cord injury (SCI) research for over 40 years and has served as Principal Investigator to various NIH awards in his career, including heading the Multicenter Animal Spinal Cord Injury Study (MASCIS), an NIH R01 multicenter grant, from 1993 to 1997. Currently Distinguished Professor of Cell Biology & Neuroscience and the Richard H. Shindell Chair in Neuroscience, Dr. Young has widespread research interests ranging from stroke, neonatal hypoxia-ischemia, Down Syndrome, and stem cells. In addition to laboratory research, Dr. Young has led many clinical trials in the United States and around the world. He is well qualified to lead the project.

Actual or anticipated problems or delays and actions or plans to resolve them

The partial closure of Rutgers laboratories in March, 2020, due to the COVID-19 pandemic, has caused some delays in completing a few of the Year 1 Major Tasks although the project team has completed most of them as well as some which were planned for completion in Year 2. The dorsal root ganglia experiments have shown that axons retracted significantly following surgical blade transection and hence end-to-end fusion was not observed. However, side-to-side axon fusion appears to occur and ongoing experiments may allow evaluation of fusogen activities.

Changes that had a significant impact on expenditures

During the time that Rutgers laboratories were partially closed from March through July, 2020, due to the COVID-19 pandemic, salaries and benefits were paid without interruption to all of the project team personnel included in the project budget. Project team members were able to continue laboratory work with some limitations imposed by Rutgers rules on personnel safety.

Significant changes in use or care of human subjects, vertebrate animals, biohazards, and/or select agents

Significant changes in use or care of human subjects

Although no significant changes were made, a blood draw protocol to obtain fresh human blood red cells for the hemolysis studies has been prepared and approved by Rutgers IRB. We are awaiting guidance from the US Army HRPO as to whether they need to approve this protocol before we initiate the studies.

Significant changes in use or care of vertebrate animals

Nothing to report.

Significant changes in use of biohazards and/or select agents

Nothing to report.

6. PRODUCTS:

- **Publications, conference papers, and presentations**

Journal publications.

Nothing to report.

Books or other non-periodical, one-time publications.

Nothing to report.

Other publications, conference papers and presentations.

Nothing to report.

- **Website(s) or other Internet site(s)**

https://sites.rutgers.edu/lbr/peripheral-nerve-regeneration-and-treatment/

- **Technologies or techniques**

Tyrosine-derived polymeric surfactants are being developed in this project for fusion of transected peripheral nerves. Many other potential applications of these block copolymer surfactants are envisioned.

- **Inventions, patent applications, and/or licenses**

As stated above, an Invention Disclosure has been submitted by Dr. David Devore and Prof. Joachim Kohn to Rutgers Innovation Ventures group for review.

- **Other Products**

The 3D printed scaffold which were developed for the study of the effects of fusogens on severed dorsal root ganglia axons may have several other potential applications.

7. PARTICIPANTS & OTHER COLLABORATING ORGANIZATIONS

What individuals have worked on the project?

Name: Joachim Kohn, PhD
Project role: PI (January-November, 2020)
Researcher Identifier:
Person-months worked: 1.0
Contribution: Planning experiments, mentoring personnel

Name: David Devore, PhD
Project role: Consultant
Researcher Identifier:
Person-months worked: 2.5
Contribution: Thermodynamic calculations, project management, preparation of annual reports

Name: Joseph Rosen, MD
Project role: Consultant
Researcher Identifier:
Person-months worked:0.2
Contribution: Review of experiments, experimental planning, clinical perspectives

Name: Antonio Merolli, MD
Project role: Co-investigator
Researcher Identifier:
Person-months worked: 2.0
Contribution: Experimental planning, perform DRG experiments and data analysis, prepare for in vivo rat surgeries, clinical perspectives

Name: Yong Mao, PhD
Project role :Research (Research Associate Professor)
Researcher Identifier:
Person-months worked: 2.0
Contribution: Performed in vitro cytotoxicity experiments, experimental planning and data review
Funding support: NJ Center for Biomaterials, Rutgers University

Name: Daniel Chakhalian, MD
Project role: Research
Researcher Identifier:
Person-months worked: 12
Contribution: Flow cytometry experiments, clinical perspectives
Funding support: NIH T-32 Fellowship Rutgers University

Name: Cemile Betkas, PhD
Project role: Research
Researcher Identifier:
Person-months worked: 12
Contribution: Design and fabrication of 3d printed scaffolds, dorsal root ganglia experiments
Funding support: NIH T-32 Fellowship, Rutgers University

Name: Kim-phuong Le, PhD
Project role: Research (Research Assistant Professor)
Researcher Identifier:
Person-months worked: 4
Contribution: Biophysical characterization of block copolymer surfactants

Name: Mariana Lima, BS
Project role: Research
Researcher Identifier:
Person-months worked: 12
Contribution: Design, synthesis and biophysical characterization of block copolymer surfactants

Name: Chrstine Gwin, BA
Project role: Research Technician
Researcher Identifier:
Person-months worked: 3
Contribution: Support of in vitro and in vivo experiments

Name: Robert Shultz, PhD
Project role: Research
Researcher Identifier:
Person-months worked: 2
Contribution: prepare dorsal root ganglia, experimental planning
Funding support: NIH T-32 Fellowship, University of Pennsylvania

Has there been a change in the active other support of the PD/PI(s) or senior/key personnel since the last reporting period?

Nothing to report

What other organizations were involved as partners?

Organization: University of Pennsylvania
Location: Philadelphia, PA
Partner's contribution: Robert Shultz, PhD, a Rutgers T-32 program postdoctoral fellow working under the mentorship of Prof. Kacy Cullen at the University of Pennsylvania, has actively participated in the project team meetings, providing valuable insights on nerve cell culture and fusogens, and he has isolated and provided ex vivo rat dorsal root ganglia for the planned experiments at Rutgers.

8. **SPECIAL REPORTING REQUIREMENTS**
   COLLABORATIVE AWARDS:
   QUAD CHARTS:

9. **APPENDICES: Appendix 1. AWARD CHART**

Award Log Number:PR192281 Award Title:W81XWH2010048/ Fusogen Nanomedicine for Peripheral Nerve Repair

PI: John Brennan, Rutgers University, NJ **Budget:** $298,962
Topic Area: FY19 PRMRP Discovery Award **Mechanism:** Funding Opportunity

Research Area(s): SCS Coding 1400 Neuroscience **Award Status: January 1, 2020 –December 31, 2021**

Study Goals: The goal of this research project is to develop a new paradigm for the treatment of traumatic nerve injuries. A thermodynamically-based understanding of polymeric fusogen activity will emerge from the structure-activity relationships obtained here. The ultimate goal is to restore motor and sensory function for trauma patients with severed peripheral nerves.

Specific Aims: Aim 1. Formulation and biophysical characterization of fusogen nanoparticles (FNPs) comprised of tyrosine-derived polymeric surfactants (TyPSs) designed and synthesized based on calculated thermodynamic properties; Aim 2. Evaluation of FNP in vitro axonal membrane repair and cytotoxicity; Aim 3. Evaluation of the lead FNP in an in vivo rat tibial nerve injury model.

Key Accomplishments and Outcomes: 1) Thermodynamic solubility parameters and hydrophile;lipophile balances (HLBs) were calculated for a wide range of TyPSs, which provided systematic estimates of TyPS ability to bind cholesterol and to interact with cell phospholipid membranes; 2) An initial set of TyPSs were synthesized based on their predicted thermodynamic properties and were demonstrated to self-assemble into functional FNPs having particle diameters appropriate for injectable nanomedicines; 3) the TyPSs inserted into Langmuir phospholipid monolayer films and their FNPs effectively bound significant levels of cholesterol; 4) the TyPS were non-cytotoxic to human dermal cells and caused the fusion of rat B35 neuroblastoma cells while improving their viability; and, 5) new methods for cutting and detecting fusion of dorsal root ganglia axons were developed.

Publications: none to date
Patents: none to date
Funding Obtained: none to date

Appendix 2. Transition Plan Questionnaire

Transition Plan Questionnaire

Directions: Please answer all questions that apply for each product under development. Please fill out one document per product.
This is not an application for funding; however, answers will help us understand the outcomes and products from your award.

1. After the award closes, would you be willing to periodically provide voluntary information (via email) regarding the project status (i.e. where the research is headed)? **Yes** ☑ or **No** ☐
These responses will help CDMRP demonstrate the return on its investments and will help demonstrate that the CDMRP is a responsible and successful steward of federal research funding.

2. What **conclusion(s)** does your final data support?

We have just entered Year 2 of our two year project. We have concluded from our work to date in Year 1 that our tyrosine-derived polymeric surfactants (TyPSs) can be designed using calculated thermodynamic properties, specifically Hansen solubility parameters and Hydrophile:Lipophile Balance (HLB), such that they effectively self-assemble into fusogen nanoparticles (FNPs) with high binding affinity for cholesterol and they strongly insert into phospholipid film models of cell membranes. The FNPs improve the viability of human dermal cells and rat neuronal cells in vitro, and depending on their specific compositions, some FNPs cause in vitro fusion of the rat neuronal cells. It is anticipated that the observed axonal fusion in vitro in the DRG model will be observed in the planned in vivo rat tibial nerve transection studies to be determined in Year 2.

3. Will you/have you applied for/obtained follow-on-funding for this project? **If yes**, please list (a) funding organization, (b) total budget requested/obtained, and (c) title of the funded proposal. ***This information will be recorded as an outcome to this award.***

Yes, we intend to seek follow-on funding and are awaiting completion of our initial in vivo rat model studies before determining the best opportunities (NIH R01 and/or DoD PRMRP funding).

4. What will be **the next step(s)** for this project?

Completion of a few remaining Year 1 Tasks which were delayed due to the partial closure of the university's laboratories because of the COVID-19 pandemic , and completion of Year 2 Tasks including in vitro dorsal root ganglia and in vivo rat model studies.

5. How would you classify your **lead candidate product**? a
(a) Therapeutic (Small Molecule, Biologic, Cell/Gene Therapy): Please choose, if applicable
(b) Diagnostic
(c) Device
(d) Research Tool to Address a Research Bottleneck
(e) Knowledge Product (Non-material product such as a compound library, database, something that improves clinical practice, education, etc.)
(f) Other - Please Specify: NANOMEDICINE

6. How does your candidate product aid the Warfighter, Veteran, Beneficiary, and/or General Population?

Peripheral nerve injuries suffered in combat are a leading cause of unfitting conditions. The fusogen approach has the potential of making a paradigm shift in how these injuries are treated and in providing substantial improvements in the restoration of nerve function.

7. Therapy / Product Development, Transition Strategies, and Intellectual Property
Describe the steps and relevant strategies required to move the candidate product (knowledge or tangible) to the next phase of development and/or commercialization. Please address any issues with intellectual property.
PIs are encouraged to explore the technical requirements and the current regulatory strategies involved in product development as well as to work with their organization's Technology Transfer Office (or equivalent regulatory/legal office), federal/international regulatory experts, to develop the transition plan and to explore developing relationships with industry, DoD advanced developers (e.g. USAMMDA), and/or other funding agencies to facilitate moving the product into the next phase.

An Invention Disclosure has been submitted to the Rutgers University Innovation Ventures group and is under review for possible patent application filing. This is expected to lead to a Provisional patent application within the next few months. Assuming that the TyPS-based fusogenic nanoparticles (FNPSs) provide effective repair of transected rat tibial nerves in the experiments planned in Year 2, subsequent pre-clinical research will include large animal in vivo studies to determine FNP dosage-safety, biodistribution, pharmacokinetics and pharmacodynamics. In addition, a cGMP manufacturing process will be established. It is likely that an ongoing clinical trial of the fusgoenic efficacy of poly(ethylene glycol) (PEG) being led by another research group may be completed by that time and a decision can be made on whether to pursue FDA 510(K) approval for a TyPS product using either PEG or Poloxamer 188 as

7. Therapy / Product Development, Transition Strategies, and Intellectual Property

Describe the steps and relevant strategies required to move the candidate product (knowledge or tangible) to the next phase of development and/or commercialization. Please address any issues with intellectual property.

PIs are encouraged to explore the technical requirements and the current regulatory strategies involved in product development as well as to work with their organization's Technology Transfer Office (or equivalent regulatory/legal office), federal/international regulatory experts, to develop the transition plan and to explore developing relationships with industry, DoD advanced developers (e.g. USAMMDA), and/or other funding agencies to facilitate moving the product into the next phase.

An Invention Disclosure has been submitted to the Rutgers University Innovation Ventures group and is under review for possible patent application filing. This is expected to lead to a Provisional patent application within the next few months. Assuming that the TyPS-based fusogenic nanoparticles (FNPSs) provide effective repair of transected rat tibial nerves in the experiments planned in Year 2, subsequent pre-clinical research will include large animal in vivo studies to determine FNP dosage-safety, biodistribution, pharmacokinetics and pharmacodynamics. In addition, a cGMP manufacturing process will be established. It is likely that an ongoing clinical trial of the fusgoenic efficacy of poly(ethylene glycol) (PEG) being led by another research group may be completed by that time and a decision can be made on whether to pursue FDA 510(K) approval for a TyPS product using either PEG or Poloxamer 188 as predicate devices, which would allow relatively rapid commercialization, or whether to use the FDA's new drug (Investigation New Drug, IND) pathway for a combination product of a TyPS-based FNP with encapsulated cholesterol. The IND pathway would require human clinical trials.